



HAL
open science

Spatio-temporal variation in stable isotope and elemental composition of key-species reflect environmental changes in the Baltic Sea

Camilla Liénart, Andrius Garbaras, Susanne Qvarfordt, Jakob Walve, Agnes Karlson

► **To cite this version:**

Camilla Liénart, Andrius Garbaras, Susanne Qvarfordt, Jakob Walve, Agnes Karlson. Spatio-temporal variation in stable isotope and elemental composition of key-species reflect environmental changes in the Baltic Sea. *Biogeochemistry*, 2022, 157 (2), pp.149-170. 10.1007/s10533-021-00865-w . hal-03875006

HAL Id: hal-03875006

<https://hal.science/hal-03875006v1>

Submitted on 3 Jan 2023

HAL is a multi-disciplinary open access archive for the deposit and dissemination of scientific research documents, whether they are published or not. The documents may come from teaching and research institutions in France or abroad, or from public or private research centers.

L'archive ouverte pluridisciplinaire **HAL**, est destinée au dépôt et à la diffusion de documents scientifiques de niveau recherche, publiés ou non, émanant des établissements d'enseignement et de recherche français ou étrangers, des laboratoires publics ou privés.

1 **Spatio-temporal variation in stable isotope and elemental composition of key-species**
2 **reflect environmental changes in the Baltic Sea**

3
4 Camilla LIÉNART^{1,2}, Andrius GARBARAS³, Susanne QVARFORDT⁴, Jakob WALVE⁴,
5 Agnes ML KARLSON^{1,4}

6 ¹ Baltic Sea Centre, Stockholm University, Stockholm, Sweden

7 ² Tvärminne Zoological Station, University of Helsinki, Hanko, Finland

8 ³ Mass Spectrometry Laboratory, Center for Physical Science and Technology, Vilnius,
9 Lithuania

10 ⁴ Department of Ecology, Environment and Plant Sciences, Stockholm University, Stockholm,
11 Sweden

12
13 Corresponding author: camilla.lienart@su.se

14 OrcID: 0000-0001-5945-9869 (CL) 0000-0002-3105-8059 (AG) 0000-0002-8330-7256 (JW)
15 0000-0001-6493-9533 (AK)

16 **Keywords:** isotope baseline, amino-acid, $\delta^{15}\text{N}$, bioindicator, long-term environmental research
17 (LTER), marine monitoring, biogeochemical cycles

18
19 **Declarations**

20 **Funding:**

21 This project on retrospective chemical analyses of archived samples was funded by the
22 Stockholm University Baltic Sea Centre and DEEP “seed” money to Agnes Karlson. The
23 monitoring programs have over the years been financed by the Swedish Environmental
24 Protection Agency and the Swedish Agency for Marine and Water Management. Part of the
25 writing process was supported by a Walter and Andrée de Nottbeck post-doctoral grant
26 awarded to Camilla Liénart.

27 **Conflict of interest:** Not applicable.

28 **Availability of data and material:** The isotope metadata generated for this study are available
29 open access at the Figshare data repository (doi: 10.6084/m9.figshare.14637804, only uploaded
30 privately until acceptance of this manuscript).

31 **Code availability:** The code generated for this study are available on request to the
32 corresponding author.

33 **Authors' contributions:** CL: Investigation, Formal Analyses, Writing-Original draft, AK:
34 Conceptualization, Funding acquisition, Formal Analyses, Writing-Reviewing and Editing
35 preparation, SQ: Investigation, Resources, Reviewing and Editing. AG: Resources, Writing-
36 Reviewing and Editing.

37 **Ethics approval:** This study was carried out in accordance with the current laws in Sweden.
38 There are no legal or ethical restrictions for invertebrates or macroalgae.

39 **Consent to participate:** All authors agreed on being co-authors of this manuscript.

40 **Consent for publication:** All authors agree on publishing the paper.

41

42 **Acknowledgments:** The monitoring program of phytobenthic communities was initiated by
43 Hans Kautsky. Thanks to Ellen Schagerström for being part of recent years' field sampling.
44 We thank Lydia Källberg Normark, Daniel Ahlström, Chiara D'agata, Adele Maciute, and
45 Andrea De Cervo for assisting with sample preparation. We thank Hans-Harald Hinrichsen,
46 who kindly provided the Baltic Sea Index (BSI) data, Siv Huseby for helping with interpreting
47 environmental data from the Bothnian Sea and Jakob Walve, who provided unpublished
48 environmental data for additional pelagic monitoring station at Askö. Thanks to Erik Smedberg
49 for helping with the GIS map. We also thank François Méric and Fabian Bergland (MSc
50 Students) for their preliminary analyses on the Askö local *Cladophora* data set. Sonja Repetti
51 is thanked for proofreading this manuscript for English language. We also would like to thank
52 an anonymous reviewer for helpful comments to improve the manuscript. The authors declare
53 there is no conflict of interest.

54

55 **Abstract**

56 Carbon and nitrogen stable isotope ratios are increasingly used to study long-term change in
57 food web structure and nutrient cycling. We retrospectively analyse elemental composition (C,
58 N and P) and stable isotopes ($\delta^{13}\text{C}$, $\delta^{15}\text{N}$) in archived monitoring samples of two important taxa
59 from the bottom of the food web; the filamentous ephemeral macroalgae *Cladophora* spp. and
60 the blue mussel *Mytilus edulis trossulus* from three contrasting regions in the Baltic Sea
61 (coastal Bothnian Sea and Baltic Proper, open sea central Baltic). The aim is to statistically
62 link the observed spatial and interannual (8-24 years' time-series) variability in elemental and
63 isotope baselines with their biomass trends and to the oceanographic monitoring data reflecting
64 the ongoing environmental changes (i.e., eutrophication and climate) in this system. We find
65 clear differences in isotope baselines between the two major Baltic Sea basins. However, the

66 temporal variation in *Mytilus* $\delta^{13}\text{C}$ was similar among regions and, at the open sea station,
67 mussels and algae $\delta^{13}\text{C}$ also correlated over time, likely reflecting a global (Suess) effect,
68 whereas $\delta^{15}\text{N}$ of both taxa varied with local and regional dissolved organic nitrogen
69 concentrations in water. $\delta^{15}\text{N}$ in source amino acids allowed detection of diazotrophic N in
70 *Mytilus*, which was masked in bulk $\delta^{15}\text{N}$. Finally, *Cladophora* N:P reflected regional nutrient
71 levels in the water while P %, which differed for both taxa, was linked to food quality for
72 *Mytilus*. This study highlights the potential of a multi-taxa and multi-stable isotope approach
73 to understand nutrient dynamics and monitor long-term environmental changes.

74 1. Introduction

75 Coastal seas are highly involved in fundamental biogeochemical processes controlling nutrient
76 and organic matter cycling (Middelburg and Herman 2007; Bouwman et al. 2013; Carstensen
77 et al. 2020). They receive nutrients and organic matter from both marine (e.g., primary
78 production) and terrestrial (e.g., riverine inputs of terrestrial material, anthropogenic outfalls)
79 origins and act as a filter between both realms (Asmala et al. 2017). In addition to climate
80 change, human activities influence nutrient cycling through eutrophication, resulting in
81 changes in both absolute values and ratios between nitrogen (N) and phosphorus (P). Major
82 changes in nutrient supply are likely to affect requirements of primary producers with regard
83 to elemental building blocks and have repercussions on processes regulating elemental
84 homeostasis of consumers (ecological stoichiometry sensu Sterner and Elser 2002), with
85 consequences for food web functioning and biogeochemical cycling.

86 Archived biological samples from environmental monitoring programs can be retrospectively
87 analyzed for elemental composition (C, N, P) and stable isotope ratios of carbon and nitrogen
88 ($\delta^{13}\text{C}$, $\delta^{15}\text{N}$) to study nutrient cycling and reconstruct food webs in relation to a changing
89 environment. Carbon isotopes provide information about ultimate carbon sources for primary
90 production (Fry and Sherr 1984). Nitrogen isotopes can be used to trace specific nitrogen
91 sources, such as anthropogenic (e.g., Connolly et al. 2013) or diazotrophic ones (Rolff 2000;
92 Karlson et al. 2015), and to quantify trophic position in consumers, if estimates of trophic
93 discrimination factors are available (Vander Zanden and Rasmussen 1999, 2001; Post et al
94 2002). Organisms at the base of the food web such as filter-feeding bivalves or grazing snails,
95 with low motility and long-life span, are commonly used as proxies for isotope baselines (i.e.,
96 the ultimate C and N sources) since they integrate intra-annual variability of nutrients (e.g.,
97 Vander Zanden and Rasmussen 1999; Post 2002) over longer time spans, several months or
98 even year(s) (e.g., Gorman et al. 2017), compared to organisms with shorter life spans such as
99 zooplankton or phytoplankton. Perennial macrophytes can be used as isotope baselines when
100 no primary consumers are available (e.g., Haubrock et al. 2020). However, perennial
101 macrophytes typically reflect nutrient sources in the water column during the growth period
102 (e.g., Savage and Elmgren 2004), hence the relatively fast turnover rates of their tissue should
103 reflect a seasonal or shorter baseline.

104 In the Baltic Sea, the suspension-feeding blue mussel, the *Mytilus edulis trossulus* species
105 complex (Kijewski et al. 2006; Stuckas et al. 2009; hereafter referred to as *Mytilus* or blue

106 mussel) and ephemeral filamentous green algae from the genus *Cladophora*, are highly
107 abundant. *Mytilus* occur in densities of up to ~100 000 individuals m⁻² (Westerbom et al. 2008)
108 and constitute, through their efficient suspension-feeding, an important link between the
109 pelagic and benthic ecosystem, promoting nutrient cycling (Kautsky and Wallentinus 1980;
110 Kautsky and Evans 1987; Attard et al. 2020). *Cladophora* is widely distributed in the Baltic
111 Sea and mainly occurs from the surface down to 1 or 2 m depths, providing food and shelter
112 for invertebrates (Snoeijs-Leijonmalm 2017). It is perennial, but overwinters as a small tuft
113 attached to shallow rocky substrates. During summer it reaches its full growth and benefits
114 from nutrient enrichment (Thybo-christesen et al. 1993). Both taxa are found throughout the
115 Baltic Sea; *Cladophora* occurs from the Bothnian Bay down to the southern Baltic Proper while
116 *Mytilus* distribution is restricted in the northernmost basin, the Bothnian bay, due to low salinity
117 levels (Kautsky and Kautsky 2000). On a smaller scale, they co-occur on hard substrates at
118 shallow depths and are often the dominant taxa based on biomass (Snoeijs-Leijonmalm 2017).
119 Isotope composition in bivalves, including *Mytilus*, is commonly used to study pelagic organic
120 matter origin (Magni et al. 2013) and its variability over time and space (Briant et al. 2018;
121 Corman et al. 2018). Bivalves are considered suitable baselines for food web studies (e.g.,
122 Abrantes and Sheaves 2009; Willis et al. 2017) and in contaminant monitoring (Karlson and
123 Faxneld 2021), while *Cladophora* is mainly used as a proxy of nutrient levels in coastal waters,
124 in the Baltic and elsewhere (Mäkinen and Aulio 1986; Planas et al. 1996).

125 The pronounced latitudinal gradients of temperature, salinity and nutrients combined with
126 eutrophication and ongoing climate change in the Baltic Sea provide an ideal study system to
127 link environmental changes to resultant food web change and ecosystem functioning. In this
128 system, retrospective chemical analyses (i.e., elemental and isotope composition) of archived
129 samples help to quantify such potential changes in biota as a consequence of their changing
130 environment. Riverine inputs of organic carbon and nutrients have increased in the recent time
131 period, especially in the Bothnian Sea (Wikner and Andersson 2012; Asmala et al. 2019), and
132 is expected to continue (Andersson et al. 2015a). In the Bothnian Sea, the N:P ratio of the
133 dissolved inorganic pool is similar to the Redfield molar ratio of 16 (ca. 13, although the slight
134 N limitation has increased in recent years; Rolff and Elfwing 2015), while it is considerably
135 lower in the Baltic Proper (ca. 4), indicating strong N limitation (Savchuk 2018). Diazotrophic
136 primary producers, such as some species of bloom forming cyanobacteria, can bypass this N-
137 limitation by directly fixing N₂. Satellite images of surface accumulations indicate that these
138 blooms have increased since the 1980s (Kahru and Elmgren 2014), and this internal N loading

139 now exceeds external loadings from rivers and atmospheric deposition in the Baltic Proper
140 (Olofsson et al. 2020). Cyanobacterial blooms benefit from denitrification and phosphate
141 release from hypoxic sediments, which exacerbate the N:P imbalance in a ‘vicious cycle’
142 (Vahtera et al. 2007). The most recent decade has also seen the regular occurrence of
143 cyanobacterial blooms in the Bothnian Sea (Olofsson et al. 2020). Salinity and temperature are
144 both lower in the Bothnian Sea compared to the Baltic Proper and are the primary factors
145 affecting species distribution, including that of *Cladophora* and *Mytilus*. Predicted increase in
146 temperature and decrease in surface salinity of the Baltic Sea (Räisänen 2017 and references
147 therein) are hence expected to affect organisms, food webs and ecosystems (Andersson et al.
148 2015a; Vuorinen et al. 2015). Recent studies have shown a decrease in mussel populations over
149 recent decades in the southern Baltic Proper, linked to increasing water temperature and
150 changes in food quantity (Franz et al. 2019; Westerbom et al. 2019) and quality (Liénart et al.
151 2020). A shift in dominance from the canopy-forming perennial macrophyte *Fucus* towards
152 opportunistic ephemeral *Cladophora* has been reported since the 1980s in different areas of the
153 Baltic Sea (Kraufvelin and Salovius 2004), likely linked to eutrophication (Kautsky et al. 1986;
154 Råberg 2004; Torn et al. 2006). However, *Fucus* recovery has been observed recently in some
155 areas (Rinne and Salovius-Laurén 2020). Nonetheless, higher temperature and declining
156 salinity promote filamentous green algae (Takolander et al. 2017) while also disadvantaging
157 *Mytilus* (Westerbom et al. 2019), suggesting climate change will enforce the shift towards
158 ephemeral macrophytes and fewer mussel beds in the Baltic.

159 Tracing C and N origin in the Baltic Sea is complex, due to multiple interacting sources,
160 especially in coastal areas. In general, eutrophication is associated with elevated $\delta^{15}\text{N}$ values,
161 for instance in Baltic Proper sediment (Voss et al. 2000). Also, sewage waters that are enriched
162 in ^{15}N are traceable in macrophytes (Savage and Elmgren 2004). However, the depleted ^{15}N
163 signal of synthetic N fertilizers used in agriculture (Bateman and Kelly 2007) can be
164 confounded with the similar signal of diazotrophic cyanobacteria (Rolff 2000), the latter
165 considered an indirect effect of eutrophication (Vahtera et al. 2007). Eutrophication can result
166 in higher $\delta^{13}\text{C}$ values in plankton and mussels due to increasing plankton biomass (Oczkowski
167 et al. 2018) with the exception of cyanobacteria (generally low $\delta^{13}\text{C}$; Rolff 2000). In the
168 Bothnian Sea, the naturally low $\delta^{15}\text{N}$ - NO_3 from pristine rivers (Voss et al. 2005) should equally
169 be reflected in relatively depleted ^{15}N baselines. Furthermore, the typically low $\delta^{13}\text{C}$ both from
170 particulate organic and dissolved inorganic terrestrial carbon (i.e., $\delta^{13}\text{C}_{\text{DIC}}$) from extensive
171 riverine input in the north (Rolff and Elmgren 2000), is similarly expected to be reflected in a

172 low $\delta^{13}\text{C}$ baseline in the Bothnian Sea. However, low temperatures and low light availability
173 (the latter from the dark, humus rich water in the north) can also result in lower $\delta^{13}\text{C}$ values for
174 macrophytes (Wiencke and Fischer 1990; Hemminga and Mateo 1996). As an additional
175 process, the global decrease in atmospheric $\delta^{13}\text{C}$ linked with fossil fuel burning over the 20th
176 century also has an influence on carbon isotope composition in the Baltic Sea (Gustafsson et
177 al. 2015). An organism's physiology (e.g., rapid growth, nutritional stress, reproductive stages)
178 can also lead to substantial isotope variability in consumers (Doi et al. 2017; Gorokhova 2018).
179 For instance, osmoregulation is an especially N-demanding process for *Mytilus* experiencing
180 low-saline conditions in the Baltic Sea (Tedengren and Kautsky 1987) and likely influences
181 ^{15}N fractionation in mussels' tissues, hence confounding the dietary origin of the $\delta^{15}\text{N}$ signal
182 (Liénart et al. 2020). To better trace ultimate N sources, the end-member $\delta^{15}\text{N}$ signal can be
183 measured in source amino acids (e.g., phenylalanine), which show negligible ^{15}N fractionation
184 during assimilation, physiological processes or trophic transfer (McClelland and Montoya
185 2002) compared to the bulk $\delta^{15}\text{N}$ signal. Finally, regarding N and P elemental composition of
186 algae and mussels, taxa-specific physiological requirements may override nutrient background
187 in the water. Fast-growing algae such as *Cladophora* are under little homeostatic control
188 compared to slow growing consumers like mussels (Smaal and Vonck 1997), and may
189 therefore better reflect basin-specific nutrient conditions.

190 The general aim of this study is to test whether eutrophication and climate-related changes are
191 mirrored in two widely distributed and abundant key taxa: the filamentous algae *Cladophora*
192 and the blue mussel *Mytilus*. This main aim is divided into three objectives: to identify (I)
193 potential region-specific differences and (II) potential consistency in temporal changes in
194 elemental and isotope baselines of these two taxa and (III) link the observed year-to-year and
195 long-term variability in the isotope and elemental data to environmental and oceanographic
196 variables, and ultimately to population level data for each taxa.

197 We expect that (1) spatially, elemental and isotope composition of both taxa will reflect the
198 latitudinal gradient in nutrients, with lower values of $\delta^{13}\text{C}$, $\delta^{15}\text{N}$, N% and P% in the more
199 oligotrophic, Bothnian Sea compared to the Baltic Proper. However, lower $\delta^{13}\text{C}$, $\delta^{15}\text{N}$, N% and
200 P% values in the Bothnian Sea of both taxa may reflect increased influence of riverine
201 (terrestrial) input in this basin; (Table S1 and Liénart et al. 2020); (2) temporally, the decrease
202 in eutrophication in recent years should be reflected in decreases in $\delta^{13}\text{C}$, $\delta^{15}\text{N}$, N% and P% in
203 our longest time series, though potential increase in riverine influence in the system is also
204 expected to lead to decreasing $\delta^{13}\text{C}$ but in increasing values of $\delta^{15}\text{N}$, N% and P% (Table S1

205 and Liénart et al. 2020); (3) N and P contents of *Cladophora* should reflect water nutrient
206 concentrations in the water earlier in the year whereas *Mytilus* should have a greater
207 homeostatic control over N and P content (and thus no link to water nutrient concentrations);
208 (4) osmotic stress, especially in the low-saline Bothnian Sea, will influence blue mussel N
209 requirements and hence confound $\delta^{15}\text{N}$ values (Lienart et al 2020). **Table S1** describe the
210 rationales for predictor selection that supports our hypotheses.

211 To explore these expectations, we take advantage of long-term oceanographic and land-based
212 monitoring data and archived biological samples for the well-studied Baltic Sea. We
213 retrospectively analyse elemental (C, N and P) and stable isotope ($\delta^{13}\text{C}$, $\delta^{15}\text{N}$) composition of
214 *Cladophora* and *Mytilus* from three contrasting regions (coastal Bothnian Sea, coastal Baltic
215 Proper and open sea Baltic Proper), in time series spanning 8 to 24 years and link these biotic
216 proxies to potential drivers. Finally, we correlate chemical, environmental and oceanographic
217 data to population level biomass data in both taxa.

218

219 **2. Material and methods**

220 **2.1. Study areas and sampling**

221 This study used data from the following study regions: 1) the Bothnian Sea coastal region
222 (Höga Kusten (HK)), 2) the Baltic Proper coastal archipelago area (Askö (A)), and 3) the Baltic
223 Proper open sea (island of Gotland (G)) (**Fig. 1**, details **Table S2**). Within the Swedish marine
224 monitoring program of the phyto-benthic community, both the blue mussels *Mytilus* and
225 filamentous green algae *Cladophora* have been sampled once a year at different stations and
226 archived over the periods 1993-2016 for A, 2000-2016 for G, and 2008-2016 for HK. These
227 taxa were sampled in three replicates (three quadrates of 20×20 cm) collected every year along
228 the same land-to-sea transects (different depths, three quadrates per depth) in late August/early
229 September by SCUBA divers. Samples were oven-dried at 60°C and stored in the dark, dry and
230 at room temperature. From each year and region, *Mytilus* individuals, n = 3 (G and HK) n = 15
231 (A), from similar size class (length: 10.0 ± 1.5 mm, mean \pm sd; **Table S2**) from 5 m depth at
232 the most exposed station in each region (two stations at HK to allow n = 3 per year; **Fig. 1**),
233 were selected for biometric and chemical analyses (details below). *Cladophora* material (a few
234 grams dry weight homogenised material, coming from many specimens) from 1 meter depth
235 was selected for chemical analysis for three to six stations per region (**Fig. 1**). The rationale
236 behind using several stations within each region for *Cladophora* was to avoid variability from

237 local nutrient conditions (such as bird guano on a particular rock), whereas one station was
238 deemed sufficient for mussels, which actively filter-feeds large amounts of water.

239 Temperature ($^{\circ}\text{C}$), salinity, dissolved inorganic nitrogen and phosphorus (DIN, DIP, $\mu\text{mol L}^{-1}$)
240 1), total nitrogen and phosphorus (total N, total P, $\mu\text{mol L}^{-1}$; i.e., includes dissolved
241 inorganic, dissolved organic, and particulate fractions), and the phytoplankton community
242 were measured by the Swedish national monitoring program for the nearby pelagic ecosystem:
243 the station C3 close to Höga Kusten, station B1 close to Askö island in Stockholm's
244 archipelago and the open sea station BY31 north of Gotland island (Fig. 1, Table S2). For more
245 details about sampling and analytical methods, see supplemental material Table S2, Andersson
246 et al. (2015b) and Liénart et al. (2020). All environmental and phytoplankton community data
247 are available at <http://www.smhi.se> (Marine environmental monitoring data - SHARK
248 database). Surface terrestrial total organic carbon transport (TOC, total loadings in tons) for
249 each watershed in Sweden is measured monthly within the freshwater monitoring program
250 "river mouths" (chemical analyses) and is available at <http://webstar.vatten.slu.se/db.html>
251 (HAVET 2015/2016).

252

253 **2.2.Elemental and isotope analysis**

254 Dry ground material from both *Cladophora* and *Mytilus* soft tissue (individual whole mussel
255 soft tissues, shells not included but weight of shells taken for later condition index calculations)
256 were used for elemental carbon, nitrogen and phosphorus (% of C, N, P expressed per dry
257 weight), bulk carbon and nitrogen isotope ($\delta^{13}\text{C}$, $\delta^{15}\text{N}$) and amino-acid- $\delta^{15}\text{N}$ measurements
258 (AA- $\delta^{15}\text{N}$). Individual specimens of *Mytilus* soft tissue were used for C and N elemental and
259 isotope measurements and P % was measured individually in different specimens, since the
260 mussels were too small for all analyses in the same individual (soft tissue was on average
261 2.1 ± 1.5 mg in mussels in this size range; Table S2). Phosphorus in *Cladophora* was only
262 measured for 4 of the 6 stations at A (not measured from Lac and StA) and 3 of the 4 stations
263 at HK (not measured for Dön). Amino-acid- $\delta^{15}\text{N}$ analysis was performed on pooled *Mytilus*
264 material (ca. 5 individuals per region and year).

265 Phosphorus analyses of individual mussels were performed at the Department of Ecology,
266 Environment and Plant Sciences (Stockholm, Sweden) using a Alpkem SFA system to analyse
267 phosphate (SS-EN ISO 15681-2:2018), after combustion and persulfate digestion, following
268 Larsson et al. (2001). C and N elemental and bulk stable isotopes were measured at the Center

269 for Physical Science and Technology (Vilnius, Lithuania) with a Flash EA 1112 Series
270 Elemental Analyzer (Thermo Finnigan) connected to a DeltaV Advantage Isotope Ratio Mass
271 Spectrometer (Thermo Fisher).

272 In order to validate ultimate nitrogen sources independently of potential physiological effect,
273 we further compared bulk $\delta^{15}\text{N}$ composition with a smaller data set of $\delta^{15}\text{N}$ in source amino
274 acids for both taxa. Amino-acid- $\delta^{15}\text{N}$ analysis of *Mytilus* was conducted at the Center for
275 Physical Science and Technology (Vilnius, Lithuania) and details are presented in
276 supplemental material. In brief, the extraction and derivatization of amino acids were
277 performed following the method described in Ledesma et al. (2020), then analysed by GC-C-
278 IRMS with a Trace GC Ultra Gas Chromatograph (Thermo scientific) coupled to a Delta
279 Advantage Isotope Ratio Mass Spectrometer via GCC III combustion interface
280 (ThermoFinnigan). *Cladophora* amino-acid- $\delta^{15}\text{N}$, which had a lower N content, was analysed
281 at the University of California Davis Stable Isotope Facility (UC Davis) following the method
282 described on <https://stableisotopefacility.ucdavis.edu/gcamino.html> (details in suppl. material).

283 All isotope data are expressed using the conventional delta notation: $\delta^{13}\text{C}_{\text{sample}}$ or $\delta^{15}\text{N}_{\text{sample}} =$
284 $[(R_{\text{sample}}/R_{\text{standard}})-1]$, where $R=^{13}\text{C}/^{12}\text{C}$ or $^{15}\text{N}/^{14}\text{N}$, with per mil deviation (‰) from
285 international standards, Vienna Pee Dee belemnite for $\delta^{13}\text{C}$ and atmospheric N_2 for $\delta^{15}\text{N}$.
286 External and internal standards were analysed as references within each batch of samples
287 (details in suppl. material). Analytical uncertainties were $<0.15\text{‰}$ and $<0.20\text{‰}$ for $\delta^{13}\text{C}$ and
288 $\delta^{15}\text{N}$ respectively and $<0.30\text{‰}$ for AA- $\delta^{15}\text{N}$. The overall analytical precision was 0.9% and
289 0.2% for elemental C and N respectively.

290

291 **2.3. Data analyses**

292 **2.3.1. Condition index and population data**

293 The Condition Index ($\text{CI}_{\text{Mytilus}} = \text{dry weight soft tissue (g)} / \text{dry weight shell (g)} \times 100$) was
294 calculated as an indicator of mussels' health status (e.g., Filgueira et al. 2013; Irisarri et al.
295 2015) on the same individual *Mytilus* used for stable isotope analysis (n.b. each mussel's soft
296 tissue and shell weight were taken separately). The N:P ratio of both taxa ($\text{N:P}_{\text{Cladophora}}$,
297 $\text{N:P}_{\text{Mytilus}}$) was calculated to be compared to Redfield ratio in the water.

298 For each station of the three regions (Fig. 1), and for each year, i) *Cladophora* total biomass (g
299 dry weight per m^2) from ca. 1 meter depth, ii) *Mytilus* total biomass (g dry weight including

300 shells per m²) and abundance (individual per m²), as well the ratio between the two
301 (Bm:Ab_{Mytilus}, mg dry weight per individual, a proxy for average mussel size in the population),
302 were calculated for all size classes (from juveniles ≥1 mm to bigger mussels >10 mm, only a
303 few individuals had a shell length exceeding 20 mm, Åkermark et al. in prep) at ca. 5 m depth.
304 Calculations for each region (average of stations) were based on geometric mean for the total
305 biomass of both taxa and the Bm:Ab_{Mytilus} ratio, to avoid influence from extreme values, and
306 on the median for *Mytilus* abundance.

307

308 2.3.2. Environmental and oceanographic data

309 For each station, environmental data were first integrated over 0-10 m depth (average) for each
310 sampling date, then averaged per month (linear interpolation was performed for missing
311 sampling dates or months). The average values per period were then calculated: the annual
312 mean (January to August 31st, i.e., approximate date of biota sampling each year) for
313 temperature, salinity, total N and P and the winter mean (January-February, i.e., reliable period
314 to measure nutrient concentrations and reflect the general conditions of each region) for DIN
315 and DIP concentrations (Table S2). The DIN:DIP ratio in the water (mol:mol) was calculated
316 for each year based on winter concentrations. The maximum summer temperature (T_{max}) was
317 considered over the period June-August for the Baltic Proper stations and July-August for the
318 Bothnian Sea (Table S2). The total biovolume (mm³ L⁻¹) of phytoplankton community (total
319 Phyto.) integrated over 0-10 m depth (multiplied by 2 at stations B1 and BY31 to adjust for the
320 tube sampling depth of 0-20m compared to the 0-10 at C3, Olofsson et al. 2020) was calculated
321 over the productive period (March-August, see details Table S2). In addition, and over the same
322 period, the biovolume of four groups representing most of the phytoplankton community
323 biomass (diatoms, dinoflagellates, cyanobacteria and the ciliate *Mesodinium rubrum*) were
324 recalculated as an integrated sum (area under the curve (AUC) linear interpolation), following
325 Liénart et al. (2020) (see details Table S2). A lag in the productive period was considered for
326 the northern station (April-August). Summer AUC values, for only cyanobacteria, were also
327 calculated to be later compared with *Cladophora* variables. Yearly averages of total organic
328 carbon loadings (TOC_{terr}, tons) were calculated from the different watersheds of each region
329 (Table S2). The average day of the year the shift in water temperature from 8 to 10-12°C
330 occurred (i.e., temperature rise triggering spawning, Kautsky pers. com.) was calculated for
331 each region (T_{shift}, in Julian days) and used as a proxy of climate change (with this shift

332 supposedly occurring earlier in recent years). Finally, to capture the variations in the Ocean-
333 Atmosphere Regime of the Baltic Sea (i.e., large-scale climatic index related to the North
334 Atlantic Oscillation), the Baltic Sea Index (BSI) was calculated according to Lehmann et al.
335 (2002).

336

337 **2.4. Statistical analysis**

338 Data treatment and statistical analysis were performed using R free software (R Core Team
339 (2020). R: A language and environment for statistical computing. R Foundation for Statistical
340 Computing, Vienna, Austria. <https://www.R-project.org/>, version 4.0.3 (2020-10-10)), except
341 for the DistLM models, which were performed in PERMANOVA+ of PRIMER version 6
342 (Anderson et al. 2008). For all statistical univariate tests, critical p -value was set to 0.05.

343

344 **2.4.1. Pre-analysis of *Cladophora* data**

345 Since *Cladophora* were sampled at 3 to 6 stations within each region, local variability in
346 elemental and isotope composition among these stations within each region was investigated
347 prior to subsequent analyses. Unidirectional trends in time series using Mann-Kendall tests
348 (details below) were explored for the individual stations within a region. Potential station effect
349 over the entire time period was tested with a Kruskal-Wallis test followed by Bonferroni
350 corrected Mann-Whitney pairwise comparison tests. Since little difference among stations was
351 found (see results 3.1.1.), the annual mean of the 3 to 6 stations was computed for each variable
352 and region for use in further analyses.

353

354 **2.4.2. Region-specific differences and temporal trends in all data sets**

355 To test for region-specific differences in elemental and isotope baselines (objective I) the last
356 9 years of each time period (Höga Kusten is only 9 years long) was compared using a Kruskal-
357 Wallis test followed by Bonferroni corrected Mann-Whitney pairwise comparison tests.

358 To test for unidirectional trends in elemental and isotope baselines (objective II) as well as in
359 the other biological and environmental variables for each region, Mann-Kendall tests were
360 used. Autocorrelation was checked (`acf()`, {stats}), and if required, a modified version of the
361 test for autocorrelated time series was applied (`mmkh3lag()`, {modifiedmk} package, version

362 1.5.0, allowing autocorrelations). To further test similarities in temporal development among
363 regions (objective II), correlations were calculated for each unique variable of the same taxa
364 over the same time series length. Correlations were evaluated, for % C, N, P, N:P_{Cladophora} with
365 Spearman's rank correlation while Pearson's correlation were used for stable isotope and
366 biometric data on *Mytilus* ($\delta^{13}\text{C}$, $\delta^{15}\text{N}$, $\text{CI}_{\text{Mytilus}}$). To test similarities between the two taxa within
367 each region, correlations (as described above) were calculated for each unique variable between
368 *Mytilus* and *Cladophora*.

369 Finally, in order to summarize the major patterns of variation among the different regions,
370 principal component analyses (PCA, scaled data) were performed for i) elemental and isotope
371 composition of *Cladophora* and *Mytilus* (separate analyses) and ii) environmental data. The
372 results of these analyses are presented in Supplemental Material.

373

374 **2.4.3. Linking biological and environmental and oceanographic data**

375 Several statistical approaches were used in order to explore linkages between the observed
376 year-to-year and long-term variability from chemical biomarkers to population level data with
377 environmental and oceanographic variables (objective III).

378 First, to identify which of the environmental variables (11 for *Cladophora*, 15 for *Mytilus*,
379 **Table S1**) are correlated to the combined dataset of elemental and isotope composition of
380 *Cladophora* or *Mytilus*, distance-based linear models were used (DistLM, resemblance matrix
381 created using Euclidean distances, evaluated using both forward and stepwise selection of
382 explanatory variables based on Akaike information criterion). The final DistLM model was
383 plotted as a redundancy analysis.

384 Second, to model the relationship between a single response variable in each taxon ($\delta^{15}\text{N}$, $\delta^{13}\text{C}$,
385 N%, P%) or the population biomass (and for *Mytilus*, the abundance and $\text{Bm:Ab}_{\text{Mytilus}}$) with the
386 environmental and phytoplankton explanatory variables (11 to 17 predictors, the rationales for
387 including predictors in the different models are presented **Table S1**, see also our general
388 expectations in the end of introduction), partial least squares regression (PLSR) were used.
389 PLSR analyses were performed on mean-centred and variance-standardized data, with models
390 optimized to two components (as detailed in Lienart et al. 2020). Selection and removal of
391 predictors were performed stepwise i) according to the variable of importance for projection
392 (VIP) scores values (with a cut-off of 0.8 Wold et al. (2001) extended to 0.9 when needed for

393 more parsimonious models i.e., ≤ 7 predictors) and ii) trying to maximize both R^2Q (indicates
394 model predictive capacity) and R^2Y (explanatory capacity, analogous to coefficient of
395 determination in regression analysis, R^2X is the explained variance). Quality of the model was
396 evaluated based on both explanatory $R^2Y > 0.6$ and predictive $R^2Q > 0.4$ capacities.
397 Standardized regression coefficients were calculated for each predictor from the two-
398 component model to ascertain the significance of environmental factors explaining and
399 predicting the variance in response variables. PLSR analyses were performed using a modified
400 version of the {pls} R package (v. 2.7-0, August 2018) as detailed in Liénart et al. (2020).

401 Finally, in order to test the direct relationship between the N:P ratio of the biota and the
402 DIN:DIP in the water of each region over time (expectation 3), linear models were applied for
403 each taxon (lm(), allowing the interaction region x N:P water). Variability in $N:P_{Cladophora}$ was
404 also investigated locally (4 stations, Fur, Str, Jus, Iss) for our longest time series only (A), using
405 distance to the shore (in km from an arbitrary runoff point selected with regard to the
406 agricultural landscape occupying the bay and its position relative to the stations), and compared
407 with the local DIN:DIP in the water (inner station, s028 and outer station s025; 2004-2016
408 August only; Fig. 1).

409

410 3. Results

411 3.1. Region specific differences in elemental and isotope baselines

412 3.1.1. Comparison of *Cladophora* within regions

413 There were no significant differences in *Cladophora* $\delta^{13}C$ and $\delta^{15}N$ between stations in any of
414 the regions with the exception of $\delta^{13}C$ in the coastal Bothnian Sea ($p = 0.05$, between Bön and
415 Sjä at Höga Kusten; Table S3, Fig. S1). There were no significant trends in any of *Cladophora*
416 elemental and isotope variables over time (Table S4). Elemental composition differed only
417 between some stations of the coastal archipelago (Askö) and the open Baltic Proper (Gotland,
418 Table S3). Thus, mean values for *Cladophora* $\delta^{13}C$ and $\delta^{15}N$ and C, N and P % were calculated
419 within regions, and used in subsequent analyses.

420

421 3.1.2. Comparisons among regions (expectation 1)

422 Both taxa had significantly higher $\delta^{15}N$ values from the Baltic Proper coastal archipelago
423 station (Askö) compared to the other regions (Fig. 2, Fig. S2, Table S5). *Cladophora* $\delta^{13}C$ was

424 lower in the coastal Bothnian Sea station (Höga Kusten) and *Mytilus* $\delta^{13}\text{C}$ was higher in the
425 open Baltic Proper station (Gotland) compared to the other regions (Fig. 2, Fig. S2, Table S5).
426 For both taxa, N % and N:P ratio did not differ between the regions and P % was generally
427 lower at Gotland compared to Höga Kusten (Fig. 2, Fig. S2, Table S5). The condition index of
428 *Mytilus* ($\text{CI}_{\text{Mytilus}}$) was significantly higher for the mussels of Höga Kusten than for the Baltic
429 Proper, and was significantly lower for Askö archipelago than for Gotland (Fig. 2, Fig. S2,
430 Table S5). Within each region, $\delta^{13}\text{C}$ and $\delta^{15}\text{N}$ were never significantly correlated for the
431 mussels nor algae (Table S6).

432 3.1.3. Ultimate nitrogen sources: $\delta^{15}\text{N}$ in amino acids for both taxa (expectation 1)

433 There was a significant correlation between bulk $\delta^{15}\text{N}$ and $\delta^{15}\text{N}$ -Phe for both taxa (*Mytilus*: p
434 = 0.028, $\rho = 0.61$; *Cladophora*: $p = 0.008$, $\rho = 0.83$, Fig. 3). Between regions, *Mytilus* $\delta^{15}\text{N}$ -
435 Phe was lowest for Gotland in the open Baltic Proper (-2.9 ± 1.6 ‰) and for Höga Kusten in the
436 coastal Bothnian Sea (-1.9 ± 0.4 ‰) and higher for the coastal archipelago of Askö (-0.7 ± 2.0
437 ‰). *Cladophora* $\delta^{15}\text{N}$ -Phe was lowest at Höga Kusten (-0.7 ± 0.03 ‰), intermediate in Gotland
438 (1.1 ± 3.5 ‰), and highest for Askö (4.6 ± 3.4 ‰, Fig. S3). Regardless of region, *Mytilus* had
439 generally negative $\delta^{15}\text{N}$ values of the source amino acid Phenylalanine ($\delta^{15}\text{N}$ -Phe) compared
440 to more positive values for *Cladophora* (Fig. 3).

441

442 3.2. Comparison between the two taxa within regions (expectation 1)

443 Regardless of region, the % P and N were higher in the mussels (N: 9.5 ± 1.0 %, P: 0.8 ± 0.1 %)
444 than in the green algae (N: 1.9 ± 0.4 %, P: 0.1 ± 0.04 %), and $\delta^{13}\text{C}$ was higher for *Cladophora* ($-$
445 15.9 ± 1.8 ‰) than *Mytilus* (-22.3 ± 0.8 ‰). $\delta^{15}\text{N}$ was generally higher for *Mytilus* (5.1 ± 1.3 ‰),
446 except for *Cladophora* from Askö, which showed high values comparable to the mussels at
447 this site (5.8 ± 1.2 ‰), but was lower in the other regions (ca. 2.0 ± 1.5 ‰) (Fig. 2). *Cladophora*
448 and *Mytilus* $\delta^{13}\text{C}$ were positively correlated at Gotland ($r = 0.65$, $p = 0.01$), and for their $\delta^{15}\text{N}$
449 values at Askö ($r = 0.41$, $p = 0.04$), while no significant correlation was observed at Höga
450 Kusten (please note $n = 9$; Table S7).

451

452 3.3. Temporal changes in elemental and isotope baselines (expectation 2)

453 Over time, *Mytilus* $\delta^{13}\text{C}$ and $\delta^{15}\text{N}$ at Askö ($\tau = -0.37$, $p = 0.01$, $\tau = -0.41$, $p = 0.005$
454 respectively) and N % at Gotland ($\tau = -0.50$, $p = 0.01$) in the Baltic Proper were significantly
455 decreasing, while no patterns in isotopes could be identified for the shorter time series of the

456 Bothnian Sea station Höga Kusten (Table S8, Fig. 2). There was no significant trend for any
457 *Cladophora* variables at the regional level (Table S8). *Mytilus* $\delta^{13}\text{C}$ was positively correlated
458 between the two coastal stations from different basins: Askö and Höga Kusten ($r = 0.82$, $p =$
459 0.01), and also between the two stations of the Baltic Proper (Gotland and Askö, $r = 0.59$, $p =$
460 0.02 ; Table S9). *Mytilus* N % was positively correlated between Gotland and Höga Kusten ($r =$
461 0.78 , $p = 0.02$; Table S9, no correlations between regions for *Cladophora* variables).

462

463 3.5. Environmental and oceanographic and population data

464 The biomass of *Cladophora* was on average similar at all regions (A: $7.7 \pm 7.6 \text{ g m}^{-2}$, G: 6.6 ± 5.4
465 g m^{-2} , HK: $5.6 \pm 4.7 \text{ g m}^{-2}$; Fig. 4, Table S8), and there was no temporal trend over time nor
466 correlation between regions (Table S8 and S9). *Mytilus* biomass was high at Askö in the coastal
467 Baltic Proper archipelago ($453 \pm 163 \text{ g m}^{-2}$), about four times lower at Gotland in the open Baltic
468 Proper ($129 \pm 43 \text{ g m}^{-2}$), and 100 times lower at Höga Kusten in the coastal Bothnian Sea (4 ± 3
469 g m^{-2} , Fig. 4, Table S8). Further details are presented in supplemental material (Fig. S4, Table
470 S5 and S8).

471 The station C3 in the Bothnian Sea was characterized by high total organic carbon loadings
472 (TOC_{terr}), low salinity and water temperature, low total nitrogen (N) and phosphorus (P), and
473 low dissolved inorganic phosphorus (DIP) concentrations (Fig. 5, Fig. S5). Generally, the
474 stations B1 and BY31, in the coastal and open Baltic Proper respectively, had higher salinity,
475 total and dissolved N and P concentrations and total phytoplankton biovolumes (total Phyto.)
476 compared to C3 (Fig. 5, Fig. S5). The station B1 was characterized by higher concentrations
477 of dissolved inorganic N (DIN), while BY31 had more dinoflagellates, N_2 -fixing cyanobacteria
478 and larger phytoplankton biovolumes (Fig. 5, Fig. S5). Over time (Fig. S5, Table S10), C3
479 showed a significant decrease in DIN:DIP. Both B1 and BY31 showed a significant increase
480 in total P and significant decrease in temperature shift (T_{shift}), indicating that the rapid
481 temperature rise from 8 to 10-12 °C is now occurring earlier in the year in the Baltic Proper.
482 Total N and phytoplankton biomass, especially dinoflagellates, significantly increased at
483 BY31. DIN, DIN:DIP and the ciliate *Mesodinium rubrum* significantly decreased and TOC_{terr}
484 significantly increased at B1. Environmental variables were rarely correlated (Table S11).

485

486 3.7. Links between elemental, isotope, population, and environmental data

487 Generally, elemental and isotope composition of *Cladophora* ($R^2_{\text{adj.}} = 0.35$) and *Mytilus* ($R^2_{\text{adj.}}$
488 $= 0.31$) were associated in the DistLM analyses with 5 environmental variables, of which three
489 were the same (DIN, salinity, T_{max} , Fig. 6, Table S12). Higher $\delta^{13}\text{C}$ values in *Cladophora* were
490 linked to high salinities and maximum water temperatures in summer (T_{max}). For *Mytilus*, high
491 $\delta^{13}\text{C}$ was linked to high dinoflagellate biovolumes. Higher $\delta^{15}\text{N}$ values were linked to high
492 dissolved inorganic nitrogen (DIN) in both *Cladophora* and *Mytilus*, driven by the high values
493 in samples from the coastal station of Askö archipelago.

494 When isotope and elemental response variables were tested separately using PLSR across
495 regions (Table 1), the $\delta^{15}\text{N}$ models of both taxa met the Lundstedt criteria (predictive capacity
496 $R^2\text{Q} > 0.4$; Lundstedt et al. 1998). In line with DistLM models, high values of $\delta^{15}\text{N}$ for both
497 taxa were explained by high DIN. High $\delta^{15}\text{N}$ in *Cladophora* was generally linked to high
498 nutrient levels (DIP, total N) and to an earlier warming of waters (T_{shift}). Large blooms of N₂-
499 fixing cyanobacteria were linked to low $\delta^{15}\text{N}$ of *Mytilus*. The condition index ($\text{CI}_{\text{Mytilus}}$) was
500 also included as a predictor in the mussel's $\delta^{15}\text{N}$ model, with better condition (high $\text{CI}_{\text{Mytilus}}$)
501 linked to lower $\delta^{15}\text{N}$. In turn, *Mytilus* condition was best explained by $\delta^{15}\text{N}$ (negative
502 relationship). It was furthermore linked to the Baltic Sea Index, a proxy for global climate
503 change, and to earlier warming of water (T_{shift}), which negatively affected the mussels'
504 condition. Higher TOC_{terr} was associated with higher $\text{CI}_{\text{Mytilus}}$. High $\delta^{13}\text{C}$ for *Cladophora* was
505 linked to high water temperature (annual and summer maximum T_{max}), high phosphorus
506 concentrations (dissolved inorganic), and high total organic carbon (TOC_{terr}), the latter a proxy
507 for low light penetration (Table S2). Low $\delta^{13}\text{C}$ in *Mytilus* was linked to high DIN, high TOC_{terr} ,
508 a proxy for food quality (i.e., degraded food; Attermeyer et al. 2018), bearing a low $\delta^{13}\text{C}$ signal,
509 Table S2), and to higher salinities as well as greater total N and P. The models for elemental
510 content for both taxa generally had low predictive and explanatory performance. High N % in
511 *Cladophora* was linked to high nutrients (DIN, DIP), and to low phytoplankton bloom (more
512 light availability, a proxy for lower competition for nutrients, Table S2). In the mussels, high
513 N % was linked to higher $\text{CI}_{\text{Mytilus}}$ and lower water temperatures, as well as earlier warming of
514 water. High P % in *Cladophora* was linked to high summer water maximum temperature, low
515 total phytoplankton bloom and low TOC_{terr} loadings (higher light availability). *Mytilus* P % was
516 positively linked to DIN and to proxies for diet quality (diatoms and dinoflagellates).

517 The simpler linear models testing for stoichiometric relationship between the elemental ratio
518 N:P of the biota and water between different regions did not show any effect for *Mytilus*.
519 However, *Cladophora* N:P was explained by region-specific differences in water nutrient

520 DIN:DIP ratio (Fig. S6). These results are supported by a local dataset from Askö archipelago,
521 where N:P_{Cladophora} is low in the inner station (Fur) compared to high values for the outer
522 archipelago (Iss, significantly higher than the inland stations), with this pattern also observed
523 for the DIN:DIP in the water between these two locations (Fig. S7). Regarding population
524 models; the *Mytilus* biomass model met the Lundstedt criteria (predictive capacity $R^2Q > 0.4$)
525 and had high explanatory power ($R^2Y \geq 50\%$; Table 1). High *Mytilus* biomass was linked to
526 high $\delta^{15}\text{N}$, high nutrient concentrations (DIN, DIP, total N) and to low TOC_{terr} .

527

528 4. Discussion

529 4.1. Spatial $\delta^{13}\text{C}$ pattern differs among taxa

530 The $\delta^{13}\text{C}$ values for *Cladophora* followed a latitudinal pattern, with most depleted values in
531 the north, in support of expectation 1. This pattern was mainly explained by physical variables:
532 the low $\delta^{13}\text{C}$ in the algae from Höga Kusten, compared with algae from the Baltic Proper, was
533 linked to low water temperature and terrestrial loading, which was our proxy for light
534 penetration but might also indicate dissolved inorganic carbon with a depleted endmember ^{13}C
535 value. Light and temperature are known to drive growth and C uptake in macrophytes, thereby
536 influencing their $\delta^{13}\text{C}$ values. Enriched ^{13}C (less negative $\delta^{13}\text{C}$) is associated with enhanced
537 photosynthetic activity in warm areas like the tropics, experiencing high irradiance, compared
538 to temperate and polar regions (Wiencke and Fischer 1990; Hemminga and Mateo 1996;
539 Stepien 2015). *Cladophora* $\delta^{13}\text{C}$ was further linked to phosphorus levels in the water (DIP),
540 which likely influence its growth condition and hence $\delta^{13}\text{C}$. In limnic systems, P is the limiting
541 factor for *Cladophora* growth (Howell 2018 and references therein) but, to our knowledge, no
542 studies have tested whether N or P limit *Cladophora* growth in the Baltic Sea.

543 The $\delta^{13}\text{C}$ of *Mytilus* showed no latitudinal pattern, but instead differed between coastal areas
544 and open sea, in contrast to expectation 1. Similarly depleted ^{13}C values were observed for the
545 two coastal stations (Askö archipelago and Höga Kusten), despite them being situated in
546 different basins. In the statistical models, low $\delta^{13}\text{C}$ was linked to higher eutrophication
547 (dissolved inorganic nitrogen: DIN) and total organic carbon loadings from land (TOC_{terr}), and
548 to lower salinity. Terrestrial or organic particles from resuspended old sediment, both bearing
549 a low $\delta^{13}\text{C}$ signal (Rolff and Elmgren 2000; Voss et al. 2000), have a higher contribution to the
550 pool of suspended particulate organic material in shallow areas (i.e., close to the coast) or at
551 the vicinity of river mouths (Liégnart et al. 2017). This signal can be mirrored in the tissues of

552 filter-feeders (Lefebvre et al. 2009; Pernet et al. 2012; Briant et al. 2018). In a recent study
553 comparing the isotope signal of benthic and pelagic food web components in different sub-
554 basins of the Baltic Sea, Kiljunen et al. (2020) found a progressive north to south ^{13}C
555 enrichment pattern in both benthic and pelagic baselines, supposedly influenced by the amount
556 of allochthonous organic material from freshwater inflows. However, it is less likely that the
557 low $\delta^{13}\text{C}$ signal of *Mytilus* from the coastal station of Askö archipelago, nearly identically to
558 Höga Kusten, can be explained by temporally similar TOC_{terr} inputs, since total organic carbon
559 loadings are 10-fold lower in the archipelago area compared to Höga Kusten. Other processes
560 are likely involved, and the significant correlation over time between $\delta^{13}\text{C}$ in mussels from
561 Askö archipelago and Gotland suggests a global driver influencing the pelagic ecosystem, such
562 as the Suess effect (Gruber et al. 1999; Quay et al 2007; Gustafsson et al. 2015, see below).
563 Despite correlation over time, higher $\delta^{13}\text{C}$ for *Mytilus* from the open sea region Gotland reflects
564 a more marine signal, less influenced by terrestrial runoff (Rolff and Elmgren 2000). An
565 explanation for the higher $\delta^{13}\text{C}$ in *Mytilus* from Gotland could be greater eutrophication of the
566 open Baltic Proper, since ^{13}C enriched values in mussels may be the result of high plankton
567 biomass (Oczkowski et al. 2018). However, since phytoplankton biomass was never selected
568 as an important predictor in our models, this explanation is less likely. In addition, P content
569 was also lowest in Gotland mussels (and algae from this region)).

570

571 **4.2. Common $\delta^{13}\text{C}$ temporal trends may reflect global environmental changes**

572 Over time, our longest dataset (1993-2016) from Askö archipelago in the coastal Baltic Proper
573 revealed a significant decrease in *Mytilus* $\delta^{13}\text{C}$, as reported in Lienart et al. (2020). A similar
574 decrease in *Mytilus* $\delta^{13}\text{C}$ was also demonstrated from the same time period in Kvädöfjärden, a
575 coastal station 100 km south of Askö archipelago (Ek et al. 2021). However, the Kvädöfjärden
576 time series was longer (starting in 1981), and there was no evident decrease when considering
577 the entire series of nearly 4 decades. Still, the nearly identical temporal variation (and absolute
578 values) in $\delta^{13}\text{C}$ for mussels from Askö archipelago and Höga Kusten, and the positive
579 correlation over time in $\delta^{13}\text{C}$ for *Mytilus* from Kvädöfjärden, Askö archipelago and Gotland,
580 suggest a large-scale effect on $\delta^{13}\text{C}$ values in recent decades (in contrast to our more local
581 expectation 2). Furthermore, even though not significant ($p < 0.08$ in both cases), the results
582 suggest a positive correlation trend between mussels and algae $\delta^{13}\text{C}$ at both Gotland and Askö
583 archipelago. This large-scale similarity in $\delta^{13}\text{C}$ over time may hence reflect common global or

584 at least northern hemisphere changes not included in our statistical approach. The worldwide
585 decrease in $\delta^{13}\text{C}$ of atmospheric CO_2 as a result of global anthropogenic activities (e.g., fossil
586 fuels use and deforestation; referred to as the Suess effect; Gruber et al. 1999; Quay et al. 2007
587 and references therein), has significantly affected marine biota over recent decades (Schloesser
588 et al. 2009). This global process is reflected in ultimate source of carbon in the Baltic Sea
589 (Gustafsson et al. 2015) and could underlie the more recent (since 1993 and onwards) decrease
590 in the $\delta^{13}\text{C}$ of phytoplankton mirrored in our mussels. We found a significant 1‰ depletion in
591 $\delta^{13}\text{C}$ values of the mussels over the 24 year time period (see calculations in suppl. material),
592 which is consistent with the decreases reported for other marine organisms (Druffel and
593 Benavides 1986; Bauch et al. 2000; Schloesser et al. 2009). Similar multi-decadal decreasing
594 trends for $\delta^{13}\text{C}$ have been observed in bivalves (including *Mytilus*) from the English Channel
595 and the Mediterranean Sea (Briant et al. 2018). A general decrease since the early 90s has also
596 been demonstrated from various organisms and for different trophic levels in coastal and
597 pelagic food webs of the in the North Sea and Baltic Sea, including Herring gull (Corman et
598 al. 2018) and Atlantic salmon (Torniainen et al. 2014).

599

600 **4.3. $\delta^{15}\text{N}$ pattern is region-specific for both taxa**

601 The high and similar $\delta^{15}\text{N}$ values of *Cladophora* and *Mytilus* from the coastal Baltic Proper
602 (Askö archipelago) were both linked to the high DIN concentration in this region. Savage and
603 Elmgren (2004) described high $\delta^{15}\text{N}$ values in *Fucus vesiculosus* close to a sewage outfall north
604 of Askö archipelago but reported that values were back to background level ($\delta^{15}\text{N}$ of 4‰)
605 towards the Askö island, 24 km away from the sewage outlet. The $\delta^{15}\text{N}$ of *Cladophora* in our
606 study, however, remained high around Askö island (ca. 6.5‰). This could be explained by the
607 higher nutrient uptake and growth rate of the seasonal filamentous algae, with a high
608 surface:volume ratio (Snoeijs-Leijonmalm 2017) compared to the slow growing perennial
609 *Fucus* spp. (Wallentinus 1984), which makes *Cladophora* a more effective N-sink. The
610 significant decrease in $\delta^{15}\text{N}$ of both taxa in the Askö archipelago over time is statistically linked
611 to the significant decrease in DIN concentration in this area, probably reflecting the general
612 decrease in land-based nutrient loadings over recent decades as a result of eutrophication
613 mitigation (Savage et al. 2010; Elmgren et al. 2015). An alternative explanation is that it mirrors
614 changes in the internal denitrification potential from increased hypoxic bottom waters since the
615 90s resulting in less DIN (Carstensen et al. 2014). Natural features such as coastal upwellings

616 of bottom water, which are frequent on the Swedish east coast of the Baltic Proper (Lehmann
617 et al. 2012), bear an enriched ^{15}N signal that can contribute to high $\delta^{15}\text{N}$ values in macrophytes
618 (Marconi et al. 2011; Viana and Bode 2013). Bivalves including *Mytilus* can also capture the
619 high $\delta^{15}\text{N}$ signal from eutrophication (Fukumori et al. 2008; Carmichael et al. 2012; Thibault
620 et al. 2020; Liénart et al. 2020) or from upwellings indirectly via plankton ingestion, as
621 observed for invertebrates in other systems (e.g., Hill and McQuaid 2008).

622 In the Askö archipelago, both bulk $\delta^{15}\text{N}$ and $\delta^{15}\text{N}$ of phenylalanine ($\delta^{15}\text{N}$ -Phe) for *Cladophora*
623 where generally high and correlated, supporting the assimilation of ^{15}N enriched nutrients in
624 this area. For *Mytilus*, there was also a positive correlation between $\delta^{15}\text{N}$ -bulk and $\delta^{15}\text{N}$ -Phe,
625 but $\delta^{15}\text{N}$ -Phe values were much lower than for *Cladophora*, demonstrating differences in
626 utilization of ultimate N sources, with negative values indicating diazotrophic N (Rolff 2000;
627 Eglite et al. 2018). Alternatively, this may indicate different turnover time of N sources
628 between these taxa. Indeed, low $\delta^{15}\text{N}$ in *Mytilus* was explained by high amounts of N_2 -fixing
629 cyanobacteria and also linked to the mussel's condition index, indicating the role of physiology
630 on bulk $\delta^{15}\text{N}$ variability in the mussels, with lower $\delta^{15}\text{N}$ indicative of better condition (Liénart
631 et al. 2020). For *Mytilus*, slow N turnover (Smaal and Vonck 1997), and hence likely large ^{15}N
632 fractionation, may confound this signal in bulk $\delta^{15}\text{N}$ values. In addition, the low salinity
633 (expectation 4) of the Baltic Sea reduces the scope for growth and affects respiration rates of
634 the mussels (Tedengren and Kautsky 1986), thus influencing N requirements and possibly
635 confounding $\delta^{15}\text{N}$ signal.

636 Cyanobacterial N supports zooplankton and deposit-feeders during summer in the Baltic
637 Proper (Karlson et al. 2015), but there is currently no published study reporting active feeding
638 of *Mytilus* on cyanobacteria. However, a recent experimental study suggests it is a relevant
639 food source for the mussels during summer (Liénart et al. in prep). At the open sea station of
640 the Baltic Proper, cyanobacterial N fixation is higher than in the coast (Olofsson et al. 2020).
641 *Mytilus* bulk $\delta^{15}\text{N}$ in this region was accordingly lower than in the Askö archipelago, better
642 resembling the low $\delta^{15}\text{N}$ -Phe in the mussels, and also lower in algae, possibly indirectly
643 utilizing leaked N of cyanobacterial origin. Negative $\delta^{15}\text{N}$ -Phe for particulate organic matter
644 in surface water of Gotland has been confirmed previously (-1.7 to -6‰, Eglite et al. 2018).
645 The large year-to-year variability in *Cladophora* bulk $\delta^{15}\text{N}$, and possibly in $\delta^{15}\text{N}$ -Phe, could
646 also reflect the occasional influence of local upwellings at the southern tip of Gotland
647 (Lehmann et al. 2012) bringing up more enriched ^{15}N waters.

648 Finally, in the Bothnian Sea Höga Kusten, the low $\delta^{15}\text{N}$ of *Cladophora* is likely related to the
649 low $\delta^{15}\text{N}$ signal of NO_3 from pristine Nordic rivers ($\delta^{15}\text{N}\text{-NO}_3$ of $0.6\pm 1.1\%$, $\delta^{15}\text{N}\text{-PON}$ of
650 $2.9\pm 2.1\%$; Voss et al. 2005). Similarly, Kiljunen et al. (2020) show increasing $\delta^{15}\text{N}$ values
651 from north to south of both pelagic and benthic baselines in the Baltic Sea, likely related to
652 eutrophication patterns. However, increased cyanobacteria blooms in the coastal zone of the
653 Bothnian Sea over the past decade (Andersson et al. 2015b; Olofsson et al. 2020) could
654 additionally contribute to the low bulk $\delta^{15}\text{N}$ and negative $\delta^{15}\text{N}\text{-Phe}$ observed in both taxa here,
655 especially in *Mytilus*.

656

657 **4.4. Different nutrient turnover rates in taxa reflect system nutrient dynamics**

658 There were no significant differences in *Cladophora* and *Mytilus* N % or N:P across regions,
659 with only P % significantly lower for both taxa in Gotland compared to the other regions (**Table**
660 **S5**). This is surprising since the overall Baltic Sea is classified as a ‘problem area’, with
661 eutrophication status rated as mostly poor for the Central Baltic/Baltic Proper compared with
662 moderate to poor for the Bothnian sea according to the HELCOM Eutrophication Assessment
663 Tool. However, the N:P ratio of *Cladophora* was statistically linked to the water N:P ratio at a
664 regional scale (simple linear model, **Fig. S6**), and this was supported at a local scale within the
665 Askö archipelago (inner versus outer stations, **Fig. S7**), in accordance with expectation 3. In
666 our PLSR models, elemental composition for *Cladophora* was mainly linked to nutrient levels
667 and, for P %, to summer maximum water temperature and phytoplankton bloom intensity, with
668 a larger bloom driving higher competition for nutrients and resulting in less light available.
669 Nutrient concentrations in the water were generally higher for the Baltic Proper stations, and
670 the DIN:DIP ratio was close to Redfield values in the Bothnian Sea (ca. 13), but N limited in
671 the Baltic Proper (ca. 6-7, **Fig. S5**). The high nutrient absorption rates of *Cladophora* to sustain
672 rapid growth during summer (Wallentinus 1984) can thus explain the correlation between the
673 algal N:P ratio and nutrient levels in the water.

674 N:P ratio in *Mytilus* did not differ among regions, despite differences in nutrients and salinity
675 (expectation 3 and 4), reflecting the relatively higher degree of homeostatic control consumers
676 have over their elemental ratios. *Mytilus* has a low N turnover (Smaal and Vonck 1997), which
677 likely explains the general absence of significant temporal trends and spatial pattern in
678 elemental content of the mussels. A high N % in the mussels, used here as a proxy for protein
679 content (Sterner and Elser 2002), was linked to higher condition index and lower temperature,

680 with negative effects of higher temperatures on protein content, as expected (see Liénart et al.
681 2020 and references therein). Resembling the $\delta^{15}\text{N}$ model, this highlights the importance of
682 physiological processes for interpreting consumers' N elemental and isotope values.
683 Nonetheless, *Mytilus* P %, used here as a proxy for growth (Elser et al. 2003), was significantly
684 lower at the open sea station (Gotland), despite the potential for highest P exposure here. Still,
685 P content was best explained by eutrophication and diet related predictors (dinoflagellates,
686 diatoms). This emphasizes the importance of food quality for the growth of the mussels (e.g.,
687 Bracken 2017), with implications for their role as an ecosystem P sink.

688

689 **4.5. From nutrients to populations: understanding population level effects**

690 Our data showed a rather similar biomass per m^2 of *Cladophora* across the Baltic Sea, even
691 though a strong year to year variability was observed within regions. There are no recent studies
692 reporting *Cladophora* distribution, biomass or chemical composition in the Baltic Sea.
693 Although *Cladophora* has been reported as increasing in the Baltic since the 1980s (Kraufvelin
694 and Salovius 2004), our data did not show any significant temporal trends in *Cladophora* over
695 the past two decades. That *Cladophora* thrive in shallow areas has been mainly discussed in
696 relation to the eutrophication-induced decline of perennial brown macroalgae *Fucus* (Kautsky
697 et al. 1986; Torn et al. 2006). The two macrophytes compete for space, light and nutrients
698 (Kautsky et al. 1986), which could explain the rather high biomass of *Cladophora* in the
699 Bothnian Sea where *Fucus* is absent due to low salinity. In our analyses, the biomass of
700 *Cladophora* was linked to large-scale environmental conditions (i.e., Baltic Sea Index), and
701 stable isotopes were also included as main predictors, with high $\delta^{15}\text{N}$ reflecting eutrophication
702 (positive correlation between $\delta^{15}\text{N}$ and DIN in the model, **Table 1**). However, the biomass
703 model had low explanatory and predictive capacities, and should be interpreted with caution.
704 Adding predictors related to top-down control, such as grazing, and biomass of competitors for
705 nutrients, like *Fucus*, and ice cover and duration would likely improve the model.

706 The biomass and abundance of *Mytilus* populations were low in the Bothnian Sea, as expected
707 due to the low salinity of this area (i.e., affect growth, Kautsky et al. 1990; Westerbom et al.
708 2002). High mussel biomass was positively linked to higher nutrient concentration (DIN, DIP),
709 with both decreasing over time as a result of eutrophication mitigation, although no
710 corresponding decrease in total phytoplankton biovolume has been shown for this time period
711 (opposite trend apparent at all regions, see **Fig. S5** and Ek et al. 2021). However, compositional

712 changes of phytoplankton have occurred (Fig. S5; Hjerne et al. 2019), which influence diet
713 quality and hence the growth or survival of mussels as discussed by Liénart et al. (2020). For
714 instance, the decrease in average mussel size (Bm:Ab_{Mytilus}) in the Baltic Proper was linked to
715 decrease in DIN but also to increase in N₂-fixing cyanobacteria blooms, a food source for
716 *Mytilus* whose quality is still debated. Finally, high biomass and large average mussel size were
717 also linked to high $\delta^{15}\text{N}$, although $\delta^{15}\text{N}$ was simultaneously linked to a lower condition index
718 in individual mussels, which is contradictory. In general, the condition index was highest for
719 the mussels at Höga Kusten. This is surprising considering the low salinity of the Baltic Proper,
720 which is already at the *Mytilus* distribution area salinity limit of 4 (Snoeijs-Leijonmalm et al.
721 2017). One ecological explanation could be related to spawning, which is characterised by
722 dramatic weight loss during early summer (up to 50%, Kautsky 1982). It is possible that
723 spawning may not occur for mussels living at the salinity margin at Höga Kusten, hence
724 resulting in a high condition index contrary to Askö archipelago mussels, which are likely now
725 undergoing two spawning events per year (Westerbom pers. com.). Experimental studies
726 testing the effects of the predictors discussed here on *Mytilus* individual growth and condition
727 are hence needed to provide a mechanistic understanding for observed population biomass
728 declines.

729 5. Conclusion

730 Our study documents large-scale and long-term patterns in elemental and isotope composition
731 in the ephemeral filamentous macroalgae *Cladophora* spp. and the suspension-feeding blue
732 mussel *Mytilus* sp., two key-taxa from the Baltic Sea. We statistically link the observed patterns
733 to environmental, oceanographical and terrestrial monitoring data. The $\delta^{15}\text{N}$ of both taxa
734 responded to regional and local drivers (mainly water nutrient concentrations), yet $\delta^{15}\text{N}$ in the
735 source amino acid Phenylalanine ($\delta^{15}\text{N}$ -Phe) revealed clear differences between algae and
736 mussels regarding ultimate N source. Diazotrophic N signal was detected in *Mytilus*, which
737 was masked in bulk $\delta^{15}\text{N}$. Clear differences in carbon isotope baselines between the two major
738 Baltic Sea basins were found: the $\delta^{13}\text{C}$ followed a latitudinal gradient for the algae, while it
739 instead differed between the coastal and open sea environment for mussels. Nonetheless,
740 mussels from the different regions had similar temporal development in $\delta^{13}\text{C}$, suggesting a
741 global driver influencing $\delta^{13}\text{C}$ dynamics in the pelagic ecosystem. Elemental composition only
742 differed among regions for P %, which was lower at the open sea station for both taxa.
743 *Cladophora* N:P reflected regional nutrient levels in the water, while *Mytilus* P % was linked
744 to food quality. This study highlights the use of a multi-taxa and combined elemental and

745 isotope approach to quantify the effects of eutrophication and climate-related environmental
746 changes in food webs and ecosystem functioning.

747 **References**

- 748 Abrantes K, Sheaves M (2009) Food web structure in a near-pristine mangrove area of the Australian
749 Wet Tropics. *Estuar Coast Shelf Sci* 82:597–607. <https://doi.org/10.1016/j.ecss.2009.02.021>
- 750 Anderson MJ, Gorley RN, Clarke KR (2008) PERMANOVA+ for PRIMER. Guide to software and
751 statistical methods. PRIMER-E: Plymouth, UK. 214 pp.
- 752 Andersson A, Högländer H, Karlsson C, Huseby S (2015b) Key role of phosphorus and nitrogen in
753 regulating cyanobacterial community composition in the northern Baltic Sea. *Estuar Coast Shelf*
754 *Sci* 164:161–171. <https://doi.org/10.1016/j.ecss.2015.07.013>
- 755 Andersson A, Meier HEM, Ripszam M, et al (2015a) Projected future climate change and Baltic Sea
756 ecosystem management. *Ambio* 44:345–356. <https://doi.org/10.1007/s13280-015-0654-8>
- 757 Asmala E, Carstensen J, Conley DJ, et al (2017) Efficiency of the coastal filter: Nitrogen and
758 phosphorus removal in the Baltic Sea. *Limnol Oceanogr* 62:S222–S238.
759 <https://doi.org/10.1002/lno.10644>
- 760 Asmala E, Carstensen J, Råike A (2019) Multiple anthropogenic drivers behind upward trends in
761 organic carbon concentrations in boreal rivers. *Environ Res Lett* 14:.
762 <https://doi.org/10.1088/1748-9326/ab4fa9>
- 763 Attard KM, Rodil IF, Berg P, et al (2020) Metabolism of a subtidal rocky mussel reef in a high-
764 temperate setting : pathways of organic C flow. *Mar Ecol Prog Ser* 645:41–45.
765 <https://doi.org/10.3354/meps13372>
- 766 Attermeyer K, Catalán N, Einarsdottir K, et al (2018) Organic carbon processing during transport
767 through boreal inland waters: Particles as important sites. *123(8):2412-2428*.
768 <https://doi.org/10.1029/2018JG004500>
- 769 Bateman AS, Kelly SD (2007) Fertilizer nitrogen isotope signatures. *Isotopes Environ Health Stud*
770 43:237–247. <https://doi.org/10.1080/10256010701550732>
- 771 Bauch D, Carstens J, Wefer G, et al (2000) The imprint of anthropogenic CO₂ in the Arctic Ocean:
772 Evidence from planktic $\delta^{13}\text{C}$ data from watercolumn and sediment surfaces. *Deep-Sea Res II*
773 47:1791-1808. [https://doi.org/10.1016/S0967-0645\(00\)00007-2](https://doi.org/10.1016/S0967-0645(00)00007-2)
- 774 Bouwman AF, Bierkens MFP, Griffioen J, et al (2013) Nutrient dynamics, transfer and retention
775 along the aquatic continuum from land to ocean: towards integration of ecological and
776 biogeochemical models. *Biogeosciences* 10:1–23. <https://doi.org/10.5194/bg-10-1-2013>
- 777 Bracken MES (2017) Stoichiometric mismatch between consumers and resources mediates the growth
778 of rocky intertidal suspension feeders. *Front Microbiol* 8:1–10.

- 779 <https://doi.org/10.3389/fmicb.2017.01297>
- 780 Briant N, Savoye N, Chauvelon T, et al (2018) Carbon and nitrogen elemental and isotopic ratios of
781 filter-feeding bivalves along the French coasts: An assessment of specific, geographic, seasonal
782 and multi-decadal variations. *Sci Total Environ* 613–614:196–207.
783 <https://doi.org/10.1016/j.scitotenv.2017.08.281>
- 784 Carmichael RH, Shriver AC, Valiela I (2012) Bivalve response to estuarine eutrophication: The
785 balance between enhanced food supply and habitat alterations. *J Shellfish Res* 31:1–11.
786 <https://doi.org/10.2983/035.031.0101>
- 787 Carstensen J, Conley DJ, Bonsdorff E, et al (2014) Hypoxia in the Baltic Sea: Biogeochemical
788 Cycles, Benthic Fauna, and Management. *Ambio* 43:26–36. [https://doi.org/10.1007/s13280-013-](https://doi.org/10.1007/s13280-013-0474-7)
789 [0474-7](https://doi.org/10.1007/s13280-013-0474-7)
- 790 Carstensen J, Conley DJ, Almroth-Rosell E, et al (2020) Factors regulating the coastal nutrient filter
791 in the Baltic Sea. *Ambio* 49:1194–1210. <https://doi.org/10.1007/s13280-019-01282-y>
- 792 Connolly RM, Gorman D, Hindell JS, et al (2013) High congruence of isotope sewage signals in
793 multiple marine taxa. *Mar Pollut Bull* 71:152–158.
794 <https://doi.org/10.1016/j.marpolbul.2013.03.021>
- 795 Corman AM, Schwemmer P, Mercker M, et al (2018) Decreasing $\delta^{13}\text{C}$ and $\delta^{15}\text{N}$ values in four coastal
796 species at different trophic levels indicate a fundamental food-web shift in the southern North
797 and Baltic Seas between 1988 and 2016. *Environ Monit Assess* 190:.
798 <https://doi.org/10.1007/s10661-018-6827-8>
- 799 Doi H, Akamatsu F, González AL (2017) Starvation effects on nitrogen and carbon stable isotopes of
800 animals: An insight from meta-analysis of fasting experiments. *R Soc Open Sci* 4:.
801 <https://doi.org/10.1098/rsos.170633>
- 802 Druffel ERM, Benavides LM (1986) Input of excess CO_2 to the surface ocean based on $^{13}\text{C}/^{12}\text{C}$ ratios
803 in a banded Jamaican sclerosponge. *Nature* 321:59–61.
- 804 Eglite E, Wodarg D, Dutz J, et al (2018) Strategies of amino acid supply in mesozooplankton during
805 cyanobacteria blooms: a stable nitrogen isotope approach. *Ecosphere* 9:e02135.
806 <https://doi.org/10.1002/ecs2.2135>
- 807 Ek C, Faxneld S, Nyberg E, et al (2021) The importance of adjusting contaminant concentrations
808 using environmental data: A retrospective study of 25 years data in Baltic blue mussels. *Sci*
809 *Total Environ* 762:.
<https://doi.org/10.1016/j.scitotenv.2020.143913>
- 810 Elmgren R, Blenckner T, Andersson A (2015) Baltic Sea management: Successes and failures. *Ambio*

811 44:335–344. <https://doi.org/10.1007/s13280-015-0653-9>

812 Elser JJ, Acharya K, Kyle M, et al (2003) Growth rate-stoichiometry couplings in diverse biota. *Ecol*
813 *Lett* 6:936–943. <https://doi.org/10.1046/j.1461-0248.2003.00518.x>

814 Filgueira R, Comeau LA, Landry T, et al (2013) Bivalve condition index as an indicator of
815 aquaculture intensity: A meta-analysis. *Ecol Indic* 25:215–229.
816 <https://doi.org/10.1016/j.ecolind.2012.10.001>

817 Franz M, Barboza FR, Hinrichsen HH, et al (2019) Long-term records of hard-bottom communities in
818 the southwestern Baltic Sea reveal the decline of a foundation species. *Estuar Coast Shelf Sci*
819 219:242–251. <https://doi.org/10.1016/j.ecss.2019.02.029>

820 Fry B, Sherr E (1984) ¹³C measurements as indicators of carbon flow in marine and freshwater
821 ecosystems. *Contrib Mar Sci* 27: 13–47.

822 Fukumori K, Oi M, Doi H, et al (2008) Bivalve tissue as a carbon and nitrogen isotope baseline
823 indicator in coastal ecosystems. *Estuar Coast Shelf Sci* 79:45–50.
824 <https://doi.org/10.1016/j.ecss.2008.03.004>

825 Gorman D, Turra A, Connolly RM, et al (2017) Monitoring nitrogen pollution in seasonally-pulsed
826 coastal waters requires judicious choice of indicator species. *Mar Poll Bul* 122:419-155.
827 <https://doi.org/10.1016/j.marpolbul.2017.06.042>

828 Gorokhova E (2018) Individual growth as a non-dietary determinant of the isotopic niche metrics.
829 *Methods Ecol Evol* 9:269–277. <https://doi.org/10.1111/2041-210X.12887>

830 Gruber N, Keeling CD, Bacastow RB, et al (1999) Spatiotemporal patterns of carbon-13 in the global
831 surface ocean and the oceanic Suess effect. *Global Biogeochem Cycles* 13:307–335

832 Gustafsson E, Mörth C-M, Humborg C, et al (2015) Modelling the ¹³C and ¹²C isotopes of inorganic
833 and organic carbon in the baltic Sea. *J Mar Sys* 148:122-130.
834 <https://doi.org/10.1016/j.jmarsys.2015.02.008>

835 Haubrock PJ, Balzani P, Britton R, et al (2020) Using stable isotopes to analyse extinction risks and
836 reintroduction opportunities of native species in invaded ecosystems. *Sci Rep* 10:21576.
837 <https://doi.org/10.1038/s41598-020-78328-9>

838 HAVET, 2015/2016. Havetrappporten/Sveriges vattenmiljö. Available from
839 <http://havsmiljoinstitutet.se/publikationer/havet/havet2015-2016>. ISSN 1654-6741

840 Hemminga MA, Mateo MA (1996) Stable carbon isotopes in seagrasses: variability in ratios and use
841 in ecological studies. *Mar Ecol Prog Ser* 140:285–298

842 Hill JM, McQuaid CD (2008) $\delta^{13}\text{C}$ and $\delta^{15}\text{N}$ biogeographic trends in rocky intertidal communities
843 along the coast of South Africa: Evidence of strong environmental signatures. *Estuar Coast Shelf*
844 *Sci* 80:261–268. <https://doi.org/10.1016/j.ecss.2008.08.005>

845 Hjerne O, Hajdu S, Larsson U, et al (2019) Climate driven changes in timing, composition and
846 magnitude of the Baltic Sea phytoplankton spring bloom. *Front Mar Sci* 6:482:1–15.
847 <https://doi.org/10.3389/fmars.2019.00482>

848 Howell ET (2018) *Cladophora* (green algae) and dreissenid mussels over a nutrient loading gradient
849 on the north shore of Lake Ontario. *J Great Lakes Res* 44:86–104.
850 <https://doi.org/10.1016/j.jglr.2017.10.006>

851 Irisarri J, Fernández-Reiriz MJ, Labarta U (2015) Temporal and spatial variations in proximate
852 composition and Condition Index of mussels *Mytilus galloprovincialis* cultured in suspension in
853 a shellfish farm. *Aquaculture* 435:207–216. <https://doi.org/10.1016/j.aquaculture.2014.09.041>

854 Kahru M, Elmgren R (2014) Multidecadal time series of satellite-detected accumulations of
855 cyanobacteria in the Baltic Sea. *Biogeosciences* 11:3619–3633. [https://doi.org/10.5194/bg-11-](https://doi.org/10.5194/bg-11-3619-2014)
856 [3619-2014](https://doi.org/10.5194/bg-11-3619-2014)

857 Karlson AML, Duberg J, Motwani NH, et al (2015) Nitrogen fixation by cyanobacteria stimulates
858 production in Baltic food webs. *Ambio* 44:413–426. <https://doi.org/10.1007/s13280-015-0660-x>

859 Karlson AML, Faxneld S (2021) Polycyclic aromatic hydrocarbons and stable isotopes of carbon and
860 nitrogen in Baltic Sea blue mussels: Time series data 1981 – 2016. *Data Br* 35:4–8.
861 <https://doi.org/10.1016/j.dib.2021.106777>

862 Kautsky (1982) Quantitative studies on gonad cycle, fecundity, reproductive output and recruitment in
863 a Baltic *Mytilus edulis* population. *Mar Biol* 68:143–160

864 Kautsky N, Evans S (1987) Role of biodeposition by *Mytilus edulis* in the circulation of matter and
865 nutrients in a Baltic coastal ecosystem. *Mar Ecol Prog Ser* 38:201–212

866 Kautsky N, Kautsky L (2000) Chapter 8. Seas at the Millennium: An environmental evaluation.
867 Charles Sheppard. Eds. Elsevier Science Ltd (19 october 2000), vol 1-3, 2415pp. ISBN-10:
868 0080432077 ISBN-13: 978-0080432076

869 Kautsky N, Kautsky H, Kautsky U, Waern M (1986) Decreased depth penetration of *Fucus*
870 *vesiculosus* (L.) since the 1940's indicates eutrophication of the Baltic Sea. *Mar Ecol Prog Ser*
871 28:1–8

872 Kautsky N, Wallentinus I (1980) Nutrient release from a Baltic *Mytilus* - red algal community and its
873 role in benthic and pelagic productivity. *Ophelia Suppl.* 1:17–30

874 Kijewski TK, Zbawicka M, Väinölä R, Wenne R (2006) Introgression and mitochondrial DNA
875 heteroplasmy in the Baltic populations of mussels *Mytilus trossulus* and *M. edulis*. Mar Biol
876 149:1371–1385. <https://doi.org/10.1007/s00227-006-0316-2>

877 Kiljunen M, Peltonen H, Lehtiniemi M, et al (2020) Benthic-pelagic coupling and trophic
878 relationships in northern Baltic Sea food webs. Limnol Oceanogr 65:1706–1722.
879 <https://doi.org/10.1002/lno.11413>

880 Kraufvelin P, Salovius S (2004) Animal diversity in Baltic rocky shore macroalgae: can *Cladophora*
881 *glomerata* compensate for lost *Fucus vesiculosus* ? Estuar Coast Shelf Sci 61:369–378.
882 <https://doi.org/10.1016/j.ecss.2004.06.006>

883 Larsson U, Hajdu S, Walve J, Elmgren R (2001) Baltic Sea nitrogen fixation estimated from the
884 summer increase in upper mixed layer total nitrogen. Limnol Oceanogr 46:811–820

885 Ledesma M, Gorokhova E, Holmstrand H, et al (2020) Nitrogen isotope composition of amino acids
886 reveals trophic partitioning in two sympatric amphipods. Ecol Evol 10:10773–10784.
887 <https://doi.org/10.1002/ece3.6734>

888 Lefebvre S, Marín Leal JC, Dubois S, et al (2009) Seasonal dynamics of trophic relationships among
889 co-occurring suspension-feeders in two shellfish culture dominated ecosystems. Estuar Coast
890 Shelf Sci 82:415–425. <https://doi.org/10.1016/j.ecss.2009.02.002>

891 Lehmann A, Krauss W, Hinrichsen HH (2002) Effects of remote and local atmospheric forcing on
892 circulation and upwelling in the Baltic Sea. Tellus A Dyn Meteorol Oceanogr 54:299–316.
893 <https://doi.org/10.3402/tellusa.v54i3.12138>

894 Lehmann A, Myrberg K, Höflich K (2012) A statistical approach to coastal upwelling in the Baltic
895 Sea based on the analysis of satellite data for 1990–2009. Oceanologia 54:369–393.
896 <https://doi.org/10.5697/oc.54-3.369>

897 Liénart C, Savoye N, Bozec Y, et al (2017) Dynamics of particulate organic matter composition in
898 coastal systems: A spatio-temporal study at multi-system scale. Prog Ocean 156:221–239.
899 <https://doi.org/10.1016/j.pcean.2017.03.001>

900 Liénart C, Garbaras A, Qvarfordt S, et al (2020) Long-term changes in trophic ecology of blue
901 mussels in a rapidly changing ecosystem. Limnol Oceanogr Ino.11633.
902 <https://doi.org/10.1002/lno.11633>

903 Magni P, Rajagopal S, Como S, et al (2013) $\delta^{13}\text{C}$ and $\delta^{15}\text{N}$ variations in organic matter pools, *Mytilus*
904 spp. and *Macoma balthica* along the European Atlantic coast. Mar Biol 160:541–552.
905 <https://doi.org/10.1007/s00227-012-2110-7>

906 Mäkinen A, Aulio K (1986) The use of *Cladophora glomerata* (Chlorophyta) to monitor levels of
907 mineral nutrients in coastal waters. Publications of the Water Research Institute 68: 160—163.

908 Marconi M, Giordano M, Raven JA (2011) Impact of taxonomy, geography, and depth on $\delta^{13}\text{C}$ and
909 $\delta^{15}\text{N}$ variation in a large collection of macroalgae. J Phycol 47:1023–1035.
910 <https://doi.org/10.1111/j.1529-8817.2011.01045.x>

911 McClelland JW, Montoya JP (2002) Trophic relationships and the nitrogen isotopic composition of
912 amino acids in plankton. Ecology 83:2173–2180. [https://doi.org/10.1890/0012-9658\(2002\)083\[2173:TRATNI\]2.0.CO;2](https://doi.org/10.1890/0012-9658(2002)083[2173:TRATNI]2.0.CO;2)

914 Middelburg JJ, Herman PMJ (2007) Organic matter processing in tidal estuaries. Mar Chem 106:127–
915 147. <https://doi.org/10.1016/j.marchem.2006.02.007>

916 Oczkowski A, Taplin B, Pruell R, et al (2018) Carbon stable isotope values in plankton and mussels
917 reflect changes in carbonate chemistry associated with nutrient enhanced net production. Front
918 Mar Sci 5:1–15. <https://doi.org/10.3389/fmars.2018.00043>

919 Olofsson M, Klawonn I, Karlson B (2020) Nitrogen fixation estimates for the Baltic Sea indicate high
920 rates for the previously overlooked Bothnian Sea. Ambio 50:203–214.
921 <https://doi.org/10.1007/s13280-020-01331-x>

922 Pernet F, Malet N, Pastoureaud A, et al (2012) Marine diatoms sustain growth of bivalves in a
923 Mediterranean lagoon. J Sea Res 68:20–32. <https://doi.org/10.1016/j.seares.2011.11.004>

924 Planas D, Maberly SC, Parker JE (1996) Phosphorus and nitrogen relationships of *Cladophora*
925 *glomerata* in two lake basins of different trophic status. Freshw Biol 35:609–622.
926 <https://doi.org/10.1111/j.1365-2427.1996.tb01772.x>

927 Post DM (2002) Using stable isotopes to estimate trophic position: models, methods, and
928 assumptions. Ecology 83:703–718. [https://doi.org/10.1890/0012-9658\(2002\)083\[0703:USITET\]2.0.CO;2](https://doi.org/10.1890/0012-9658(2002)083[0703:USITET]2.0.CO;2)

930 Quay P, Sonnerup R, Stutsman J, et al (2007) Anthropogenic CO_2 accumulation rates in the North
931 Atlantic Ocean from changes in the $^{13}\text{C}/^{12}\text{C}$ of dissolved inorganic carbon. Global Biogeochem
932 Cycles 21:1–15. <https://doi.org/10.1029/2006GB002761>

933 R Core Team (2020). R: A language and environment for statistical computing. R Foundation for
934 Statistical Computing, Vienna, Austria. <https://www.R-project.org/>, version 4.0.3 (2020-10-10)

935 Råberg S (2004) Competition from filamentous algae on *Fucus vesiculosus* - negative effects and the
936 implications on biodiversity of associated flora and fauna. Plant Ecology, vol. 4. Licentiate
937 Thesis. Department of Botany, Stockholm University, pp. 1–26.

- 938 Räisänen J (2017) Future climate change in the Baltic Sea region and environmental impacts. in H V
939 Storch (ed.) , Oxford Research Encyclopedias : Climate Science . Oxford University Press ,
940 Oxford . <https://doi.org/10.1093/acrefore/9780190228620.013.634>
- 941 Rinne H, Salovius-laurén S (2020) The status of brown macroalgae *Fucus* spp. and its relation to
942 environmental variation in the Finnish marine area, northern Baltic Sea. *Ambio* 49:118–129.
943 <https://doi.org/10.1007/s13280-019-01175-0>
- 944 Rolff C (2000) Seasonal variation in delta C-13 and delta N-15 of size-fractionated plankton at a
945 coastal station in the northern Baltic proper. *Mar Ecol Ser* 203:47–65.
946 <https://doi.org/10.3354/meps203047>
- 947 Rolff C, Elfving T (2015) Increasing nitrogen limitation in the Bothnian Sea, potentially caused by
948 inflow of phosphate-rich water from the Baltic Proper. *Ambio* 44:601–611.
949 <https://doi.org/10.1007/s13280-015-0675-3>
- 950 Rolff C, Elmgren R (2000) Use of riverine organic matter in plankton food webs of the Baltic Sea.
951 *Mar Ecol Prog Ser* 197:81–101
- 952 Savage C, Elmgren R (2004) N values trace decrease in sewage influence. *Ecol Appl* 14:517–526.
953 <https://doi.org/10.1890/02-5396>
- 954 Savage C, Leavitt PR, Elmgren R (2010) Effects of land use, urbanization, and climate variability on
955 coastal eutrophication in the Baltic Sea. *Limnol Oceanogr* 55:1033–1046.
956 <https://doi.org/10.4319/lo.2010.55.3.1033>
- 957 Savchuk OP (2018) Large-Scale Nutrient Dynamics in the Baltic Sea, 1970–2016. *Front Mar Sci* 5:1–
958 20. <https://doi.org/10.3389/fmars.2018.00095>
- 959 Schloesser RW, Rooker JR, Louchuarn P, et al (2009) Interdecadal variation in seawater $\delta^{13}\text{C}$ and
960 $\delta^{18}\text{O}$ recorded in fish otoliths. *Limnol Oceanogr* 54:1665–1668.
961 <https://doi.org/10.4319/lo.2009.54.5.1665>
- 962 Smaal AC, Vonck APMA (1997) Seasonal variation in C, N and P budgets and tissue composition of
963 the mussel *Mytilus edulis*. *Mar Ecol Prog Ser* 153:167–179. <https://doi.org/10.3354/meps153167>
- 964 Snoeijs-Leijonmalm P, Schubert H, Radziejewska T (2017) Biological oceanography of the Baltic
965 Sea. Netherlands: Springer, p. 683. doi:10.1007/978-94-007-0668-2
- 966 Stepien CC (2015) Impacts of geography, taxonomy and functional group on inorganic carbon use
967 patterns in marine macrophytes. *J Ecol* 103:1372–1383. [https://doi.org/10.1111/1365-](https://doi.org/10.1111/1365-2745.12451)
968 [2745.12451](https://doi.org/10.1111/1365-2745.12451)
- 969 Sterner RW, Elser JJ (2002) Ecological stoichiometry, the biology of elements from molecules to the

- 970 biosphere. Princeton Univ. Press, Princeton, NJ
- 971 Stuckas H, Stoof K, Quesada H, Tiedemann R (2009) Evolutionary implications of discordant clines
972 across the Baltic *Mytilus* hybrid zone (*Mytilus edulis* and *Mytilus trossulus*). *Heredity* (Edinb)
973 103:146–156. <https://doi.org/10.1038/hdy.2009.37>
- 974 Takolander A, Cabeza M, Leskinen E (2017) Climate change can cause complex responses in Baltic
975 Sea macroalgae : A systematic review. *J Sea Res* 123:16–29.
976 <https://doi.org/10.1016/j.seares.2017.03.007>
- 977 Tedengren M, Kautsky N (1987) Comparative stress response to diesel oil and salinity changes of the
978 blue mussel, *Mytilus edulis* from the baltic and north seas. *Ophelia* 28:1–9.
979 <https://doi.org/10.1080/00785326.1987.10430800>
- 980 Thibault M, Duprey N, Gillikin DP, et al (2020) Bivalve $\delta^{15}\text{N}$ isoscapes provide a baseline for urban
981 nitrogen footprint at the edge of a World Heritage coral reef. *Mar Pollut Bull* 152:110870.
982 <https://doi.org/10.1016/j.marpolbul.2019.110870>
- 983 Thybo-christesen M, Rasmussen MB, Blackburn TH (1993) Nutrient fluxes and growth of
984 *Cladophora sericea* in a shallow Danish bay. *Mar Ecol Prog Ser* 100:273–281
- 985 Torn K, Krause-jensen D, Martin G (2006) Present and past depth distribution of bladderwrack
986 (*Fucus vesiculosus*) in the Baltic Sea. *Aquat Bot* 84:53–62.
987 <https://doi.org/10.1016/j.aquabot.2005.07.011>
- 988 Torniaainen J, Vuorinen PJ, Jones RI, et al (2014) Migratory connectivity of two Baltic Sea salmon
989 populations: retrospective analysis using stable isotopes of scales. *ICES J Mar Sci* 71:336–344.
990 <https://doi.org/10.1093/icesjms/fst153>
- 991 Vahtera E, Conley DJ, Gustafsson BG, et al (2007) Internal ecosystem feedbacks enhance nitrogen-
992 fixing cyanobacteria blooms and complicate management in the Baltic Sea. *Ambio* 36:186–94
- 993 Vander Zanden MJ, Rasmussen JB (1999) Primary consumer $\delta^{13}\text{C}$ and $\delta^{15}\text{N}$ and the trophic position
994 of aquatic consumers. *Ecology* 80(4):1395-1404. [https://doi.org/10.1890/0012-9658\(1999\)080\[1395:PCCANA\]2.0.CO;2](https://doi.org/10.1890/0012-9658(1999)080[1395:PCCANA]2.0.CO;2)
- 995
- 996 Vander Zanden MJ, Rasmussen JB (2001) Variation in $\delta^{13}\text{C}$ and $\delta^{15}\text{N}$ trophic fractionation:
997 Implications for aquatic food web studies. *Limnol Oceanogr* 46:2061–2066.
998 <https://doi.org/10.4319/lo.2001.46.8.2061>
- 999 Viana IG, Bode A (2013) Stable nitrogen isotopes in
1000 coastal macroalgae: Geographic and anthropogenic variability. *Sci Total Environ* 443:887–895.
<https://doi.org/10.1016/j.scitotenv.2012.11.065>
- 1001 Voss M, Emeis KC, Hille S, et al (2005) Nitrogen cycle of the Baltic Sea from an isotopic

1002 perspective. *Global Biogeochem Cycles* 19:1–15. <https://doi.org/10.1029/2004GB002338>

1003 Voss M, Larsen B, Leivuori M, Vallius H (2000) Stable isotope signals of eutrophication in Baltic Sea
1004 sediments. *J Mar Syst* 25:287–298. [https://doi.org/10.1016/S0924-7963\(00\)00022-1](https://doi.org/10.1016/S0924-7963(00)00022-1)

1005 Vuorinen I, Hänninen J, Rajasilta M, et al (2015) Scenario simulations of future salinity and
1006 ecological consequences in the Baltic Sea and adjacent North Sea areas-implications for
1007 environmental monitoring. *Ecol Indic* 50:196–205. <https://doi.org/10.1016/j.ecolind.2014.10.019>

1008 Wallentinus I (1984) Comparison of nutrient uptake rates for Baltic macroalgae with different thallus
1009 morphologies. *Mar Biol* 80:215–225

1010 Westerbom M, Kilpi M, Mustonen O (2002) Blue mussels, *Mytilus edulis*, at the edge of the range:
1011 population structure, growth and biomass along a salinity gradient in the north-eastern Baltic
1012 Sea. *Mar Biol* 140:991–999. <https://doi.org/10.1007/s00227-001-0765-6>

1013 Westerbom M, Mustonen O, Jaatinen K, et al (2019) Population Dynamics at the Range Margin:
1014 Implications of Climate Change on Sublittoral Blue Mussels (*Mytilus trossulus*). *Front Mar Sci*
1015 6:1–10. <https://doi.org/10.3389/fmars.2019.00292>

1016 Westerbom M, Mustonen O, Kilpi M (2008) Distribution of a marginal population of *Mytilus edulis*:
1017 responses to biotic and abiotic processes at different spatial scales. *Mar Biol* 135:1153–1164.
1018 <https://doi.org/10.1007/s00227-007-0886-7>

1019 Wiencke C, Fischer G (1990) Growth and stable carbon isotope composition of cold-water
1020 macroalgae in relation to light and temperature. *Mar Ecol Prog Ser* 65:283–292

1021 Wikner J, Andersson A (2012) Increased freshwater discharge shifts the trophic balance in the coastal
1022 zone of the northern Baltic Sea. *Glob Chang Biol* 18:2509–2519. <https://doi.org/10.1111/j.1365-2486.2012.02718.x>

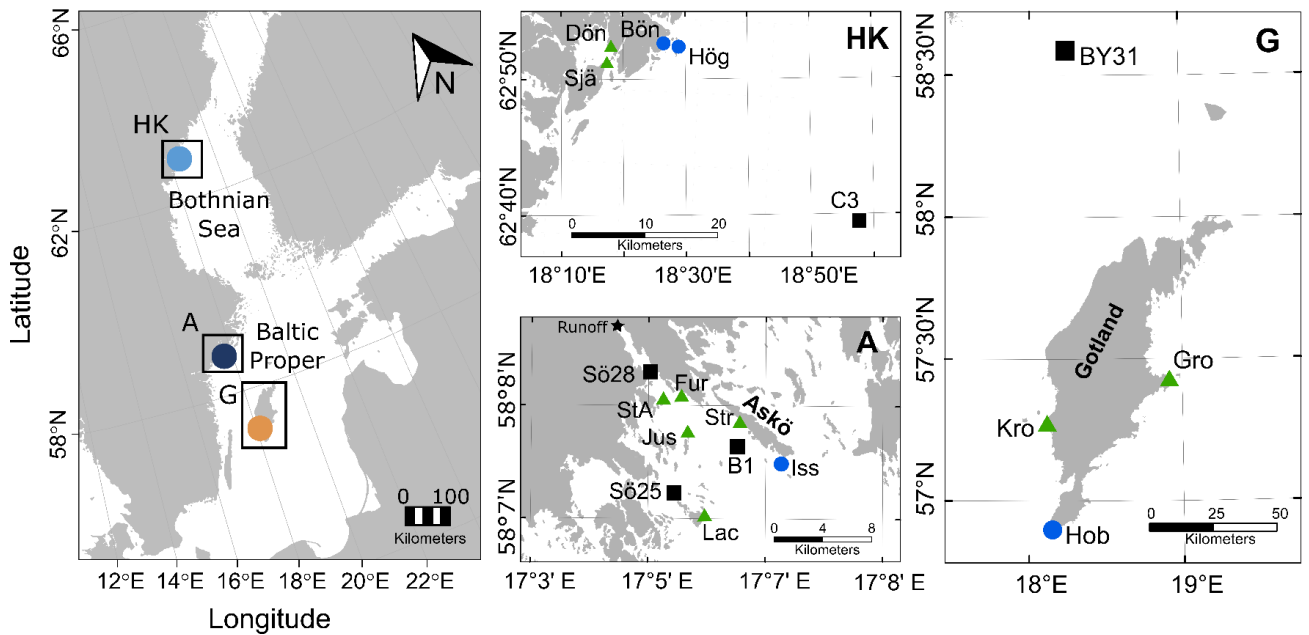
1024 Willis T V, Wilson KA, Johnson BJ (2017) Diets and stable isotope derived food web structure of
1025 fishes from the inshore Gulf of Maine. *Estuaries and Coasts* 40:889–904.
1026 <https://doi.org/10.1007/s12237-016-0187-9>

1027 Wold S, Sjöström M, Eriksson L (2001) PLS-regression: a basic tool of chemometrics. *Chemom Intell*
1028 *Lab Syst* 58:109–130. [https://doi.org/10.1016/S0169-7439\(01\)00155-1](https://doi.org/10.1016/S0169-7439(01)00155-1)

1029

1030

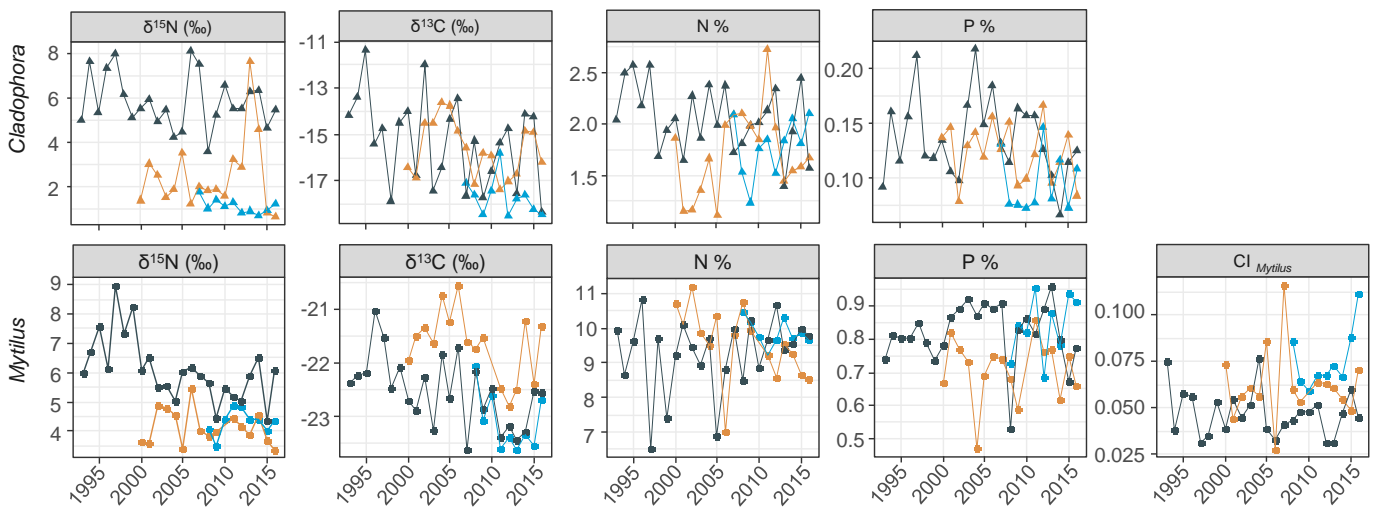
1031 **Figures and table**



1032

1033 Figure 1: Study regions of the Bothnian Sea (HK: Höga Kusten) and the Baltic Proper (A:
 1034 Archipelago close to Askö field station, and G: Gotland island). Stations within each region
 1035 are shown in the three right panels: green triangles are *Cladophora* sampling stations only, blue
 1036 circles are *Mytilus* and *Cladophora* sampling stations, black squares are pelagic environmental
 1037 monitoring stations.

1038

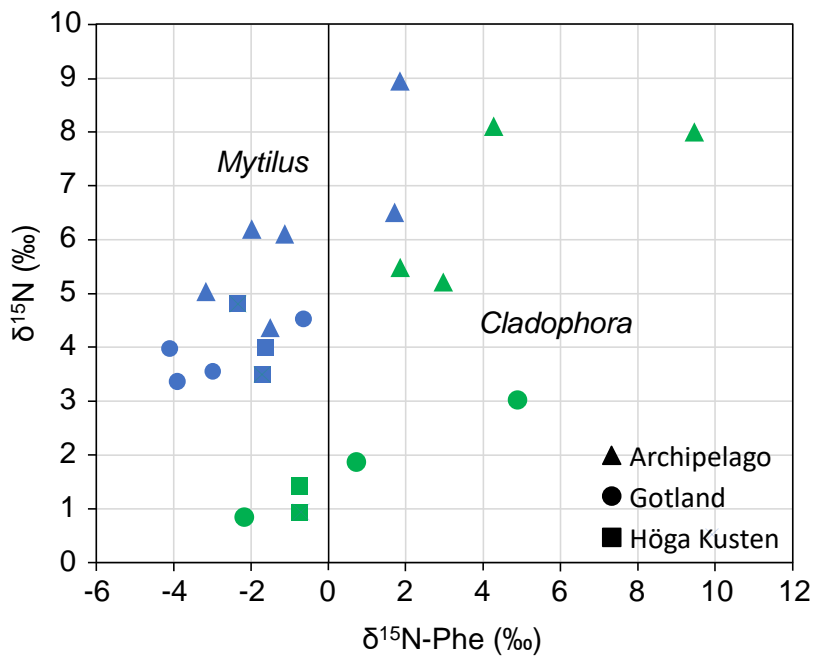


1039

1040 Figure 2: Temporal trends in elemental and isotope composition of *Cladophora* (upper panels,
 1041 triangles) and *Mytilus* (lower panels, circles) from the 3 regions (Archipelago: black, Gotland:
 1042 orange, Höga Kusten: blue). For a multivariate summary of region-specific pattern see Fig S2.

1043

1044

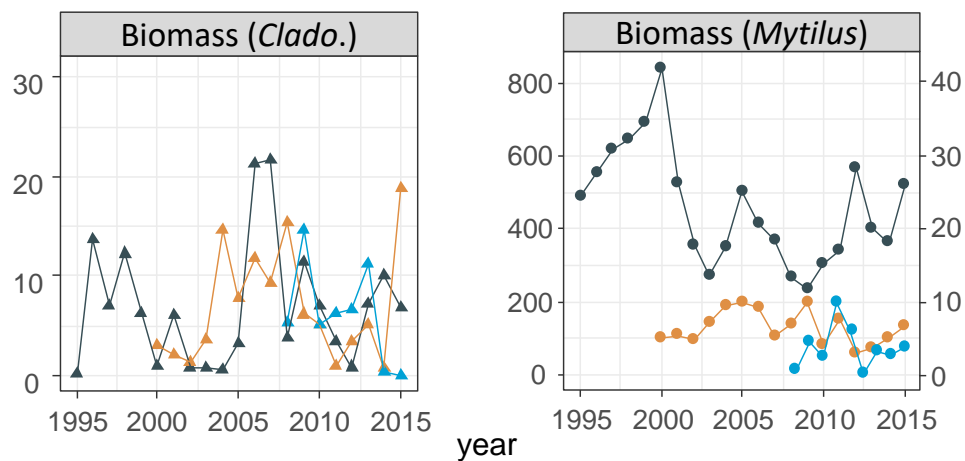


1045

1046 Figure 3: Nitrogen isotope ratio of the source amino-acid phenylalanine ($\delta^{15}\text{N}$ -Phe) for *Mytilus*
1047 (*Mytilus* (blue) and *Cladophora* (green) of the 3 regions.

1048

1049

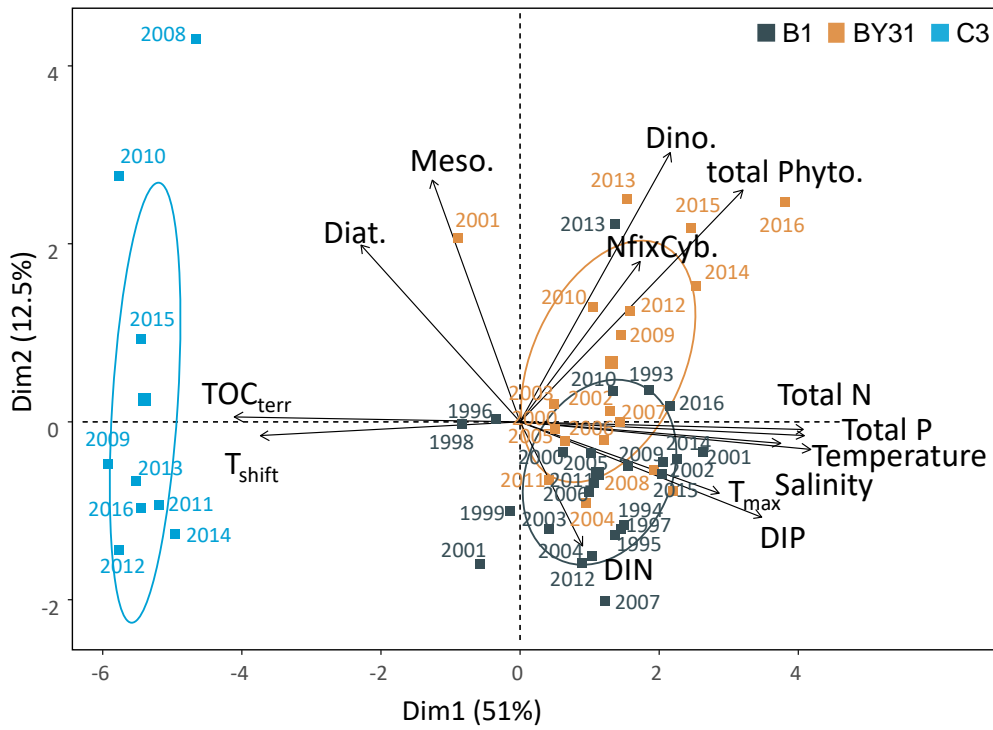


1050

1051 Figure 4: Temporal trends in *Cladophora* (triangles) and *Mytilus* (circles) population biomass
1052 (g dry weight per m²) from the 3 regions (Archipelago: black, Gotland: orange, Höga Kusten:

1053 blue). For *Mytilus* biomass, the left axis indicates Askö archipelago and Gotland and the axis
 1054 on the right indicates Höga Kusten.

1055

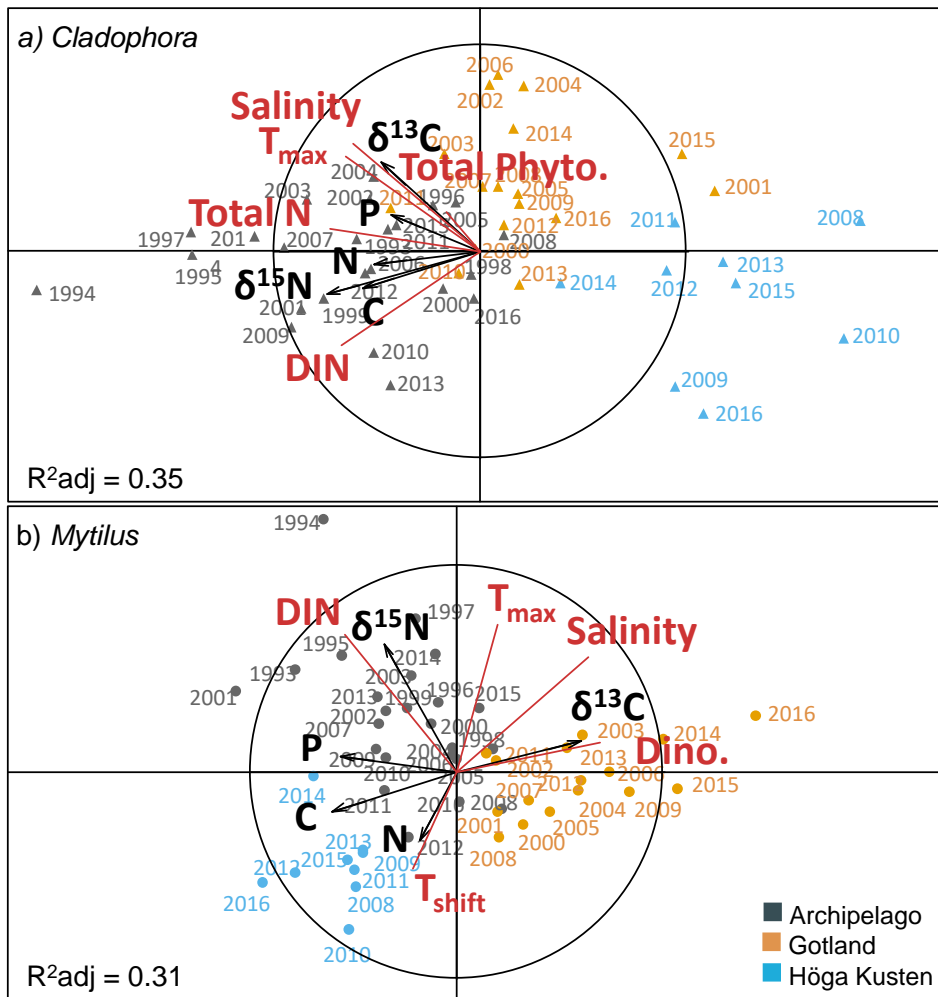


1056

1057 Figure 5: Principal component analysis (PCA) of environmental variables for B1 (black), BY31
 1058 (orange) and C3 (blue). Scaled data. Ellipses represent 50% of the data. See Fig. S5 for the raw
 1059 dataset over time. T_{max}: water maximum temperature in summer, DIN or DIP: Dissolved
 1060 Inorganic Nitrogen / Phosphorus, TOC_{terr}: total organic carbon from land, T_{shift}: water
 1061 temperature shift, Diat.: diatom, Dino.: dinoflagellates, Meso.: *Mesodinium rubrum*, NfixCyb.:
 1062 N₂-fixing cyanobacteria.

1063

1064



1065

1066 Figure 6: Redundancy analysis of a) *Cladophora* and b) *Mytilus* elemental and isotope data
 1067 (black arrows) for the 3 studied regions (Archipelago: black, Gotland: orange, Höga Kusten:
 1068 blue) constrained by environmental variables (red vectors) selected from the DistLM models
 1069 based on Akaike information criterion. DIN: dissolved inorganic nitrogen, total Phyto.: total
 1070 phytoplankton bloom, T_{max}: water maximum temperature in summer, Dino.: dinoflagellates,
 1071 T_{shift}: water temperature shift. See [Table S12](#) for model selection.

1072

1073

1074

1075

1076

1077 Table 1: Results of the PLSR models for the 6 *Cladophora* and 8 *Mytilus* response variables
1078 tested (in white: individual level, in dark grey: population level). R²Y is the model explanatory
1079 capacity, R²Q is the model predictive capacity, R²X is the explained variance. Models with
1080 high prediction capacity according to Lundstedt evaluation criteria (Lundstedt et al. 1998; R²Y
1081 > 0.6 and R²Q > 0.4) are in bold. Shaded grey cells are predictors with negative influence. The
1082 ‘-’ sign means no additional predictors. Predictors are ranked by importance based on absolute
1083 value of regression coefficient (in italics). CI_{Mytilus}: condition index, Abund.: abundance,
1084 Temp.: water temperature, T_{max}: maximum summer water temperature, T_{shift}: water
1085 temperature shift, DIP and DIN: dissolved inorganic nitrogen or phosphorus, TOC_{terr}: total
1086 organic carbon loadings, Tot. Phyto.: total phytoplankton biomass, NfixCyb.: N₂-fixing
1087 cyanobacteria, Diat.: diatoms, Dino.: dinoflagellates, BSI: Baltic Sea Index.

Response variable		Model evaluation parameters			Predictors (reg. coefficients)						
		R ² Y	R ² Q	R ² X	1	2	3	4	5	6	7
$\delta^{13}\text{C}$	<i>Cladophora</i>	0.4	0.3	0.8	T _{max} <i>0.92</i>	Temp. <i>0.32</i>	DIP <i>0.14</i>	Total P <i>-0.09</i>	Salinity <i>-0.08</i>	TOC _{terr} <i>0.06</i>	Total N <i>-0.05</i>
		0.6	0.5	0.9	DIN <i>0.92</i>	DIP <i>0.29</i>	T_{shift} <i>-0.27</i>	Total N <i>0.24</i>	Total P <i>-0.07</i>	Salinity <i>0.04</i>	-
		0.3	0.2	0.8	DIN <i>0.12</i>	DIP <i>0.08</i>	Tot. Phyto <i>-0.05</i>	Total N <i>0.02</i>	-	-	-
		0.3	0.2	0.8	Tot. Phyto <i>-0.01</i>	T _{max} <i>0.007</i>	Salinity <i>0.004</i>	TOC _{terr} <i>-0.004</i>	-	-	-
		0.2	0.0	0.7	$\delta^{15}\text{N}$ <i>1.26</i>	BSI <i>-1.25</i>	$\delta^{13}\text{C}$ <i>-0.93</i>	Total N <i>0.77</i>	DIP <i>0.61</i>	-	-
$\delta^{15}\text{N}$	<i>Mytilus</i>	0.4	0.3	0.9	DIN <i>-0.31</i>	Total P <i>0.11</i>	Salinity <i>0.10</i>	TOC _{terr} <i>-0.08</i>	Total N <i>0.02</i>	-	-
		0.6	0.5	0.8	DIN <i>0.59</i>	CI_{Mytilus} <i>-0.49</i>	NfixCyb. <i>-0.28</i>	-	-	-	-
		0.2	0.1	0.8	CI _{Mytilus} <i>0.35</i>	T _{shift} <i>-0.18</i>	T _{max} <i>-0.08</i>	Total N <i>0.01</i>	-	-	-
		0.3	0.2	0.7	DIN <i>0.025</i>	Dino. <i>-0.017</i>	Total P <i>-0.016</i>	Diat. <i>0.014</i>	Salinity <i>-0.013</i>	-	-
		0.4	0.3	0.7	$\delta^{15}\text{N}$ <i>-0.005</i>	BSI <i>0.004</i>	Total N <i>-0.003</i>	T _{shift} <i>0.002</i>	TOC _{terr} <i>0.002</i>	Salinity <i>-0.001</i>	-
		0.7	0.7	0.8	$\delta^{15}\text{N}$ <i>75</i>	DIN <i>68</i>	DIP <i>41</i>	Total N <i>29</i>	TOC_{terr} <i>-24</i>	-	-
		0.6	0.5	0.8	DIN <i>-2638</i>	$\delta^{13}\text{C}$ <i>2635</i>	Total P <i>2320</i>	Salinity <i>2238</i>	TOC_{terr} <i>-1827</i>	-	-
0.6	0.5	0.8	$\delta^{15}\text{N}$ <i>0.007</i>	NfixCyb. <i>-0.007</i>	DIN <i>0.005</i>	-	-	-	-		